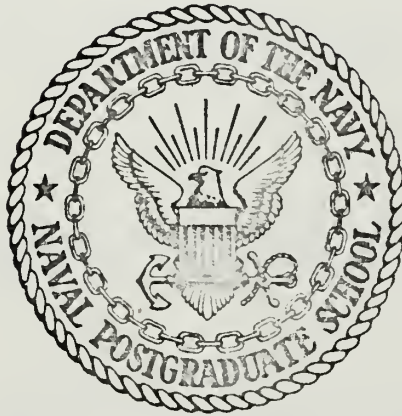


WAVE INTERACTION WITH LARGE SUBMERGED
OBJECTS

Peter Klaus Bowden

NAVAL POSTGRADUATE SCHOOL

Monterey, California



THESIS

WAVE INTERACTION
WITH LARGE SUBMERGED OBJECTS

by

Peter Klaus Bowden

December 1971

Approved for public release; distribution unlimited.

Wave Interaction with Large Submerged Objects

by

Peter Klaus Bowden
Lieutenant, United States Navy
B.S., United States Naval Academy, 1964

Submitted in partial fulfillment of the
requirements for the degree of

MASTER OF SCIENCE IN MECHANICAL ENGINEERING

from the

NAVAL POSTGRADUATE SCHOOL
December 1971

ABSTRACT

The practical and rigorous solutions of the potential problem associated with the harmonic oscillation of a submerged rigid body of arbitrary shape is presented. The use of Green's function reduces the determination of the potential to the solution of an integral equation. The integral equation is solved numerically and the dependency of the hydrodynamic quantities such as added mass and damping coefficients of the object on the frequency of the oscillation is established.

Several checks are made on the numerical results. These include the Haskind's relations check, an energy check for the radiation problem, and comparisons with closed form solutions. All the checks and comparisons are successful and it appears that the numerical procedure employed yields valid and accurate results.

TABLE OF CONTENTS

I.	INTRODUCTION - - - - -	11
II.	THEORETICAL CONSIDERATIONS - - - - -	14
	A. A REVIEW OF WAVE FORCES ON SUBMERGED OBJECTS - - - - -	-14
	B. REPRESENTATION OF THE POTENTIAL - - - - -	-21
	C. NUMERICAL SOLUTION - - - - -	24
	D. HYDRODYNAMIC FORCES AND MOMENTS - - - - -	-25
	E. HASKIND'S RELATIONS AND ENERGY CHECK - - - - -	27
III.	COMPUTER PROGRAM - - - - -	30
IV.	DISCUSSION OF RESULTS - - - - -	-36
	A. VERTICAL CYLINDER - - - - -	-36
	B. SPHEROID - - - - -	43
	C. HASKIND'S RELATIONS AND ENERGY CHECK - - - - -	54
V.	CONCLUSIONS - - - - -	-57
	APPENDIX - - - - -	58
	LIST OF REFERENCES - - - - -	68
	INITIAL DISTRIBUTION LIST - - - - -	-69
	FORM DD 1473 - - - - -	70

LIST OF TABLES

Table		Page
1	Damping Coefficients in Heave for a Submerged Sphere - - - - -	53
2	Damping Coefficients in Heave for a Floating Sphere - - - - -	-53

LIST OF FIGURES

Figure		Page
1	Definition Sketch - - - - -	15
2	Computer Program Flow Chart - - - - -	31
3	Comparison of Computer Values for Equations (22) and (24), $a = 0.2$ - - - - -	33
4	Comparison of Computer Values for Equations (22) and (24), $a = 1.0$ - - - - -	34
5	Comparison of Computer Values for Equations (22) and (24), Large Values of a - - - - -	35
6	Definition Sketch - - - - -	37
7	Horizontal Wave Force Coefficient for a Vertical Circular Cylinder - - - - -	39
8	Horizontal Wave Moment Coefficient for a Vertical Circular Cylinder - - - - -	40
9	Hydrodynamic Force Coefficient for a Vertical Circular Cylinder - - - - -	41
10	Hydrodynamic Moment Coefficient for a Vertical Circular Cylinder - - - - -	42
11	Coefficient of Damping for a Surging Sphere - - - - -	44
12	Coefficient of Damping for a Heaving Sphere - - - - -	45
13	Coefficient of Added Mass for a Surging Sphere - - - - -	46
14	Coefficient of Added Mass for a Heaving Sphere - - - - -	47
15	Horizontal Wave Force Coefficient for a Floating Sphere - - - - -	48
16	Vertical Wave Force Coefficient for a Floating Sphere - - - - -	49

Figure		Page
17	Wave Force Coefficients for a Submerged Sphere - - - - -	51
18	Hydrodynamic Force Coefficients for a Submerged Sphere - - - - -	52
19	Percent Deviation of Haskind's Relations from Diffraction Theory for a Vertical Circular Cylinder - - - - -	55
20	Percent Deviation of Haskind's Relations from Diffraction Theory for a Spheroid - - - - -	56
21	Region of Application of Green's Theorem - - - - -	59
22	Plan View of the Spheroid - - - - -	67

NOMENCLATURE

Symbol	Description
\bar{a}	characteristic length of object
a	wavelength parameter, $a = 2\pi\bar{a}/\bar{L}$, dimensionless
C_i	wave force or moment coefficient in the i^{th} direction, dimensionless
$d\bar{s}$	elementary dimensional surface area
ds	elementary dimensionless surface area
E_i	energy transmitted over one period
f_j, f	distribution function, dimensionless
F_i	wave force or moment component in the i^{th} direction, dimensionless
g	acceleration of gravity
G	Green's function
\bar{h}	water depth
h	relative depth of water, dimensionless
h_j	functions defined by (19), dimensionless
\bar{H}	wave height
Im	imaginary part
n_x, n_y, n_z	unit normal vectors, dimensionless
P'	dynamic pressure associated with the wave interaction with the fixed object
P_j	dynamic pressure associated with the i^{th} mode of oscillation, dimensionless
\bar{q}	fluid velocity vector
Re	real part
\bar{r}	plan polar coordinate
r	plane polar coordinate, dimensionless

Symbol	Description
r_1	horizontal distance between points (x,y,z) and (ξ,η,ζ) , dimensionless
\bar{s}	surface area of the object
s	surface area of the object, dimensionless
t	time
T	wave period
u_o	velocity potential for incident wave, dimensionless
u_j	velocity potentials for the radiation and scatter problems, dimensionless
\bar{X}_i°	amplitude of motion in i^{th} direction
X_i°	amplitude of linear or angular motion, dimensionless
$\bar{x}, \bar{y}, \bar{z}$	spacial variables
x, y, z	spacial variables, dimensionless
C_{ij}	i^{th} component of force or moment coefficient associated with the j^{th} component of oscillation of the object
F_{ij}	i^{th} component of the dynamic force or moment due to the j^{th} mode of oscillation
\bar{M}_{ij}	added mass coefficient
M_{ij}	added mass coefficient, dimensionless
\bar{N}_{ij}	damping coefficient
N_{ij}	damping coefficient, dimensionless
δ	Dirac delta function
ξ, η, ζ	rectangular Cartesian coordinates, dimensionless
θ	plane polar coordinate
θ_j	angular displacement of oscillating object
v	$= \sigma^2 \bar{a} / g = a \tanh (ah)$
ρ_1	$= (\xi^2 + \zeta^2)^{1/2}$

Symbol	Description
σ	angular frequency, $\sigma = 2\pi/T$
ϕ_0	velocity potential for incident wave
ϕ_j	velocity potential for oscillation of object or scatter
ϕ'	total velocity potential for diffraction problem

Subscripts

i, j	used to denote either the mode or oscillation (or scatter) or the direction of a force or moment component, depending on context
--------	--

ACKNOWLEDGEMENTS

The author wishes to thank Dr. C. J. Garrison of the Naval Postgraduate School, his advisor, for the suggestion of and his invaluable assistance in this study. He also gratefully thanks Annette, Julie and Cara for their encouragement and understanding.

I. INTRODUCTION

The need for the utilization of the natural resources imbedded in coastal waters has led to the need for greater knowledge of the interaction of surface gravity waves with large submerged objects such as oil storage tanks and pipelines. A new problem arises in the case of large bodies immersed in shallow water, the scattering of the incident wave and the free surface effect become an important consideration in the calculation of wave forces on fixed objects and hydrodynamic forces produced by oscillation of the body in otherwise still water.

The analysis which considers these two factors has come to be known as diffraction theory. In this approach separation and viscous effects may be neglected, as was confirmed by Sarpkaya and Garrison [1], provided the amplitude of the motion is sufficiently small. The problem is set up in terms of a velocity potential and the potential function is determined by use of a source distribution. The pressure on the immersed surface can be found once the source strengths are known by use of Bernoulli's equation and the resulting forces and moments are determined from the pressure distribution by surface integration.

Recently, Garrison and Seetharama Rao [2] worked out an analysis for wave interaction with submerged objects based on linear diffraction theory and applied the analysis to calculate

wave forces acting on a submerged hemisphere. They showed that for small values of the wave height to sphere diameter ratio, the wave force coefficients can be well represented by the diffraction theory and correlated as functions of the parameters, $2\pi\bar{a}/\bar{L}$ and \bar{h}/\bar{a} where \bar{h} denotes the water depth, \bar{a} the sphere radius, and \bar{L} the wave length.

Aside from the wave force problem, an additional problem may be considered which is referred to as the "radiation problem." This involves the effect of a rigid body in calm water undergoing forced harmonic oscillations in its various degrees of freedom. Of interest here are the hydrodynamic forces which may be characterized by the coefficients of added mass, added moment of inertia, and damping. Although often solved independently, the diffraction and radiation problems may be solved concurrently because they are mathematically similar.

Relations which eliminate the need to solve the problem of wave diffraction past an object by solving the forced-oscillation problem in still water were developed by M. D. Haskind in 1957. They relate the force and moment components of the diffraction problem to the asymptotic velocity potentials for the corresponding radiation problem. That is, if the waves produced by the oscillation of an object in still water are known, Haskind's relations may be used to obtain the wave forces (or moments) produced by surface waves interacting with the same object held fixed.

Conservation of energy dictates that a balance must exist between the energy required to oscillate an object, and the wave energy transmitted by surface waves across some control volume surrounding the object but at a large radial distance. The energy required to oscillate the object is directly related to the damping coefficient, and the damping coefficient may be obtained by integration of the pressure over the immersed surface. In view of conservation of energy this same energy appears at a large distance from the object in the form of radiated wave energy. Therefore, the damping coefficient may be obtained by accounting for this energy flux. The comparison of this coefficient obtained from these two methods, i.e., the near field and far field solutions, provides a valuable check on the accuracy of the numerical results generated.

The application of Haskind's relations and energy considerations to calculate wave forces on large submerged objects is the purpose of this thesis. A computer program was developed to carry out the numerical calculations and to compare the results with those from diffraction and radiation theory.

II. THEORETICAL CONSIDERATIONS

A. A REVIEW OF WAVE FORCES ON SUBMERGED OBJECTS

Consider a rigid body of arbitrary shape having a characteristic size \bar{a} submerged in water of depth \bar{h} as illustrated in Fig. 1. It is assumed that the amplitude of the motion of the fluid is sufficiently small in relation to the size, \bar{a} , that viscous effects can be neglected. The object may or may not be in contact with the free surface or the bottom. The problem set forth herein deals with the fluid motion and forces induced by the small amplitude oscillation of the object in its six degrees of freedom as well as the fluid motion associated with the interaction of the fixed object with a train of regular waves.

The small amplitude oscillatory motion of the body with frequency about its equilibrium position is described by the relationships

$$\bar{X}_i(t) = \bar{X}_i^{\circ} \operatorname{Re}[e^{-i\sigma t}] , \quad i = 1, 2, 3 \quad (1a)$$

$$\theta_i(t) = \theta_i^{\circ} \operatorname{Re}[e^{-i\sigma t}] , \quad i = 4, 5, 6 \quad (1b)$$

where \bar{X}_i° denotes the amplitude of motion in translational oscillation and θ_i° denotes the amplitude of motion in rotational oscillation. The subscript $i = 1, 2, 3$ corresponds to oscillation in the \bar{x} , \bar{y} , \bar{z} direction, respectively, and $i = 4, 5, 6$ corresponds to angular oscillation about axes

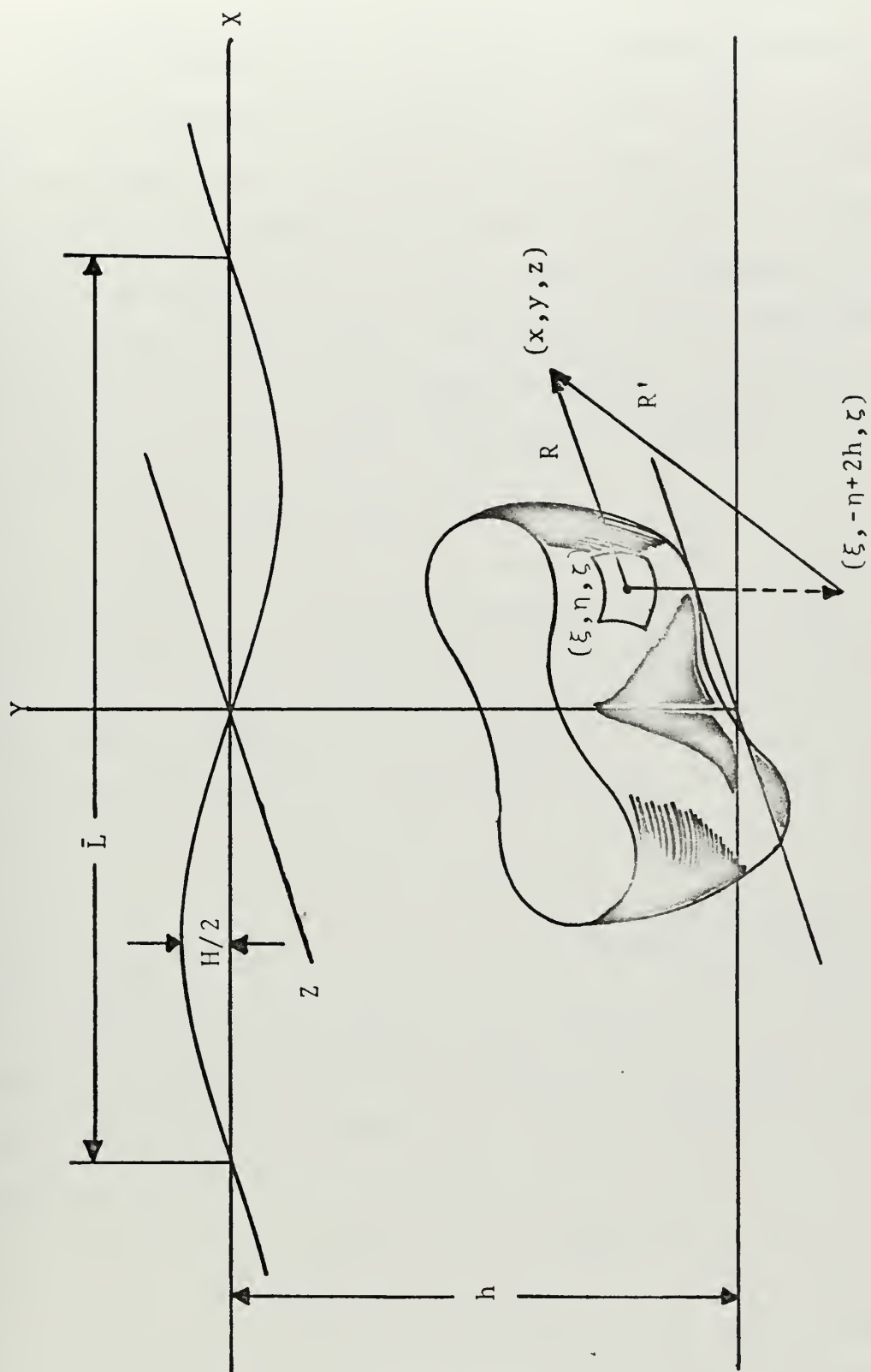


Figure 1: Definition Sketch

passing through the origin of the object parallel to the \bar{x} , \bar{y} , \bar{z} axes, respectively. The second problem considered here is the interaction of a train of regular surface waves with the object fixed in space. The incident waves of wave height \bar{H} and wave length \bar{L} are assumed to progress in the positive x-direction and the fluid motion is assumed to be incompressible, irrotational, and harmonic with time dependence $e^{-i\sigma t}$ in all cases. Consequently, a velocity potential exists such that the fluid velocity vector may be defined as

$$\bar{q}_i = \text{Re}[\bar{\nabla}\phi_i e^{-i\sigma t}] , i = 1, 2, \dots 6 \quad (2)$$

where ϕ_i denotes the velocity potential associated with the motion induced by oscillations in the six degrees of freedom. In the case of regular wave interaction with the fixed object, the velocity potential is given by the sum

$$\phi' = \phi_0 + \phi_7 \quad (3)$$

where ϕ_0 denotes the velocity potential of the incident wave in the absence of the object and ϕ_7 denotes the velocity potential of the scattered wave due to the presence of the rigid body. For this case, the fluid velocity vector is given by

$$q' = \text{Re}[\bar{\nabla}(\phi_0 + \phi_7)e^{-i\sigma t}] . \quad (4)$$

Having assumed irrotationality of the fluid, ϕ_i must satisfy the continuity equation which takes the form of the Laplace equation,

$$\nabla^2 \phi_i = 0 \quad (5)$$

within the fluid region.

Assuming that the amplitude of the motion is small, the velocity squared terms in Bernoulli's equations may be neglected. Therefore, the dynamic pressure is given as

$$P_j = \text{Re}[\rho\sigma\phi_j e^{-i\sigma t}], j = 1, 2, \dots, 6 \quad (6)$$

For the second problem, involving wave interaction with the fixed object, the pressure is given by

$$P' = \text{Re}[\rho\sigma(\phi_0 + \phi_7)e^{-i\sigma t}] \quad (7)$$

The velocity potential must satisfy certain boundary conditions in addition to Eq. (5). These include the linearized free surface boundary condition,

$$\frac{\partial \phi_j}{\partial \bar{y}}(\bar{x}, 0, \bar{z}) - \frac{\sigma^2}{g} \phi_j(x, 0, z) = 0, j = 1, 2, \dots, 7, \quad (8)$$

as well as the kinematic boundary condition on the bottom,

$$\frac{\partial \phi_j}{\partial \bar{y}}(\bar{x}, -\bar{h}, \bar{z}) = 0, i = 1, 2, \dots, 7. \quad (9)$$

Since ϕ_0 satisfies both Eqs. (8) and (9), it follows, therefore, that ϕ_7 must also satisfy these conditions.

In addition, ϕ_j must satisfy the boundary condition on the surface of the body defined by $s(\bar{x}, \bar{y}, \bar{z}) = 0$. This condition states that for an impermeable boundary, the normal velocity of the fluid must just equal the velocity of the surface normal to itself. In the case of oscillation of the

rigid body, the kinematic boundary conditions on the surface of the object take the form

$$\begin{aligned}
 \frac{\partial \phi_1}{\partial \bar{n}} (x, y, z, t) &= \dot{\bar{x}}_1^{\circ} n_x \\
 \frac{\partial \phi_2}{\partial \bar{n}} (x, y, z, t) &= \dot{\bar{x}}_2^{\circ} n_y \\
 \frac{\partial \phi_3}{\partial \bar{n}} (x, y, z, t) &= \dot{\bar{x}}_3^{\circ} n_z \\
 \frac{\partial \phi_4}{\partial \bar{n}} (x, y, z, t) &= \dot{\bar{\theta}}_4 [(\bar{h} + \bar{y}) n_z - \bar{x} n_y] \\
 \frac{\partial \phi_5}{\partial \bar{n}} (x, y, z, t) &= \dot{\bar{\theta}}_5 [\bar{z} n_x - \bar{x} n_z] \\
 \frac{\partial \phi_6}{\partial \bar{n}} (x, y, z, t) &= \dot{\bar{\theta}}_6 [\bar{x} n_y - (\bar{h} + \bar{y}) n_x]
 \end{aligned} \tag{10}$$

where $\bar{n} = \hat{i}n_x + \hat{j}n_y + \hat{k}n_z$ denotes the unit normal vector on the surface of the object directed outward into the fluid. For the case of the interaction of regular waves with a fixed, rigid body the normal velocity must be zero which may be written

$$\frac{\partial \phi_7}{\partial \bar{n}} (\bar{x}, \bar{y}, \bar{z}, t) = - \frac{\partial \phi_0}{\partial \bar{n}} (\bar{x}, \bar{y}, \bar{z}, t) . \tag{11}$$

Finally, the velocity potential must satisfy the radiation condition which permits only an outgoing progressive wave at a large distance. Hence it is required that ϕ_j have the

asymptotic form which satisfies

$$\phi_j(\bar{r}, \theta, \bar{y}) - A_j(\theta) \bar{r}_1^{-1/2} \frac{\cosh[k(\bar{h} + \bar{y})]}{\cosh(k\bar{h})} e^{i(k\bar{r}_1 - \sigma t)} \rightarrow 0 \text{ as } \bar{r}_1 \rightarrow \infty \quad (12)$$

$j = 1, 2, \dots, 7$ where $\bar{r}_1 = (\bar{x}^2 + \bar{z}^2)^{1/2}$ and $\theta = \arctan(\bar{z}/\bar{x})$

where $A_j(\theta)$ is some unknown complex function of θ .

The wave number is defined as $k = 2\pi/\bar{L}$ where \bar{L} is the wave length and is related to the frequency of disturbance according to

$$\frac{\sigma^2}{k} = k \tanh(k\bar{h}) . \quad (13)$$

The velocity potential of the incident wave alone progressing in the positive x -direction is given by

$$\phi_0(\bar{x}, \bar{y}, \bar{z}) = - \frac{ig\bar{\eta}^\circ}{\sigma} \frac{\cosh[k(\bar{h} + \bar{y})]}{\cosh(k\bar{h})} e^{-ik\bar{x}} \quad (14)$$

where $\bar{\eta}^\circ = H/2$ represents the amplitude of the incident wave, H being the wave height.

In carrying out the solution and to show more clearly the dependence of the solution on the relative wave length parameter, $a = 2\pi\bar{a}/\bar{L} = k\bar{a}$, and relative depth, $h = \bar{h}/\bar{a}$, \bar{a} being a typical length of the body, it is convenient to make the space variables and amplitudes dimensionless, i.e.,

$$x = \bar{x}/\bar{a} , y = \bar{y}/\bar{a} , z = \bar{z}/\bar{a} , r = \bar{r}/\bar{a}$$

$$X_i^\circ = \bar{X}_i^\circ/\bar{a} , i = 1, 2, 3 \text{ and } X_i^\circ = \theta_i^\circ , i = 4, 5, 6$$

and then to introduce the pressure function u_j by

$$\begin{aligned} i\sigma\phi_j(\bar{x}, \bar{y}, \bar{z})/g\bar{a}\bar{x}_j^{\circ} &= a \tanh(ah) u_j(x, y, z), \quad j = 1, 2, \dots, 6 \\ i\sigma\phi_0(\bar{x}, \bar{y}, \bar{z})/g\bar{a}\bar{n}^{\circ} &= -au_0(x, y, z) \\ i\sigma\phi_7(\bar{x}, \bar{y}, \bar{z})/g\bar{a}\bar{n}^{\circ} &= -au_7(x, y, z) . \end{aligned} \quad (15)$$

The complex dimensionless dynamic pressure amplitude can now be written by use of the linearized form of Bernoulli's equation as

$$\begin{aligned} p_j &= a \tanh(ah) u_j(x, y, z), \quad j = 1, 2, \dots, 6 \\ p' &= \frac{\cosh[a(h + y)]}{\cosh(ah)} e^{-iax} - au_7(x, y, z) \end{aligned} \quad (16)$$

where the complex amplitude of the pressure p is defined as

$$\begin{aligned} \frac{p_j}{\rho g \bar{a} \bar{x}_j^{\circ}} &= \text{Re}[p_j e^{-i\sigma t}] \\ \frac{p'}{\rho g \bar{a} \bar{n}^{\circ}} &= \text{Re}[p' e^{-i\sigma t}] \end{aligned} \quad (17)$$

The boundary value problem which describes the fluid motion arising from the oscillation of the rigid body in its six degrees of freedom as well as the scattering of the incident wave can now be written concisely in terms of dimensionless parameters. The potential $u_j(x, y, z)$, $j = 1, 2, \dots, 7$, continuous in the fluid region is sought such that

$$\nabla^2 u_j(x, y, z) = 0 \quad \text{in } y < 0 \quad (a) \quad (18)$$

$$\frac{\partial u_j}{\partial y}(x, 0, z) - a \tanh(ah) u_j(x, 0, z) = 0 \quad (b)$$

$$\frac{\partial u_j}{\partial y}(x, -h, z) = 0 \quad \text{outside } s(x, y, z) = 0 \quad (c)$$

$$\frac{\partial u_j}{\partial n}(x, y, z) = h_j(x, y, z) \quad \text{on } s(x, y, z) = 0 \quad (d)$$

$$u_j(r, \theta, y) - D_j(\theta) r_1^{-1/2} \frac{\cosh[a(h+y)]}{\cosh(ah)} e^{iar_1} \rightarrow 0 \quad \text{as } r_1 \rightarrow \infty \quad (e)$$

where $D_j(\theta)$ is some dimensionless complex function of θ , $s(x, y, z) = 0$ represents the surface of the object in its undisturbed position and h_j denotes the prescribed function which depends on the mode of oscillation ($j = 1, 2, \dots, 6$); the subscript 7 corresponds to scattering of the regular incident wave due to the presence of the rigid body. For the six degrees of freedom and scattering, the functions h_j are given, respectively, by

$$\begin{aligned} h_1 &= n_x, & h_2 &= n_y, & h_3 &= n_z \\ h_4 &= (h+y)n_z - zn_y, & h_5 &= zn_x - xn_z, & h_6 &= xn_y - (h+y)n_x \\ h_7 &= \frac{1}{\cosh(ah)} [n_y \sinh[a(h+y)] + in_x \cosh[a(h+y)] e^{iax} . \end{aligned} \quad (19)$$

B. REPRESENTATION OF THE POTENTIAL

The solution to the boundary value problem (18) may be attained by use of a Green's function having the physical interpretation of a point wave source of unit strength. These sources are distributed over the surface of the object

according to the source strength function f so that the potential at some point x, y, z within the fluid is given by the surface integral

$$u_j = \frac{1}{4\pi} \iint_S f(\xi, \eta, \zeta) G(x, y, z; \xi, \eta, \zeta) ds \quad (20)$$

where (ξ, η, ζ) represents coordinates on the surface of the object, $f(\xi, \eta, \zeta)$ represents a distribution or weighting function and $ds = d\bar{s}/\bar{a}^2$ denotes the dimensionless surface area element.

The Green's function is defined, therefore, as the function which satisfies

$$\nabla^2 G(x, y, z; \xi, \eta, \zeta) = \delta(x - \xi) \delta(y - \eta) \delta(z - \zeta) \quad (21)$$

where δ is the Dirac delta function, as well as the boundary conditions (18b, c, e). Such a function is given by Wehausen and Laitone [3] as

$$G(x, y, z; \xi, \eta, \zeta) = \frac{1}{R} + G^*(x, y, z; \xi, \eta, \zeta) \quad (22)$$

where

$$\begin{aligned} G^*(x, y, z; \xi, \eta, \zeta) = & \frac{1}{R^*} \\ & + 2P.V. \int_0^\infty \frac{(\mu + \nu) e^{-\mu h} \cosh[\mu(h + \eta)] \cosh[\mu(h + y)]}{\mu \sinh(\mu h) - \cosh(\mu h)} J_0(\mu r) d\mu \\ & + i \frac{2\pi(a^2 - \nu^2) \cosh[a(h + \eta)] \cosh[a(h + y)]}{a^2 h - \nu^2 h + \nu} J_0(ar) \end{aligned} \quad (23)$$

$$R = [(x - \xi)^2 + (y - \eta)^2 + (z - \zeta)^2]^{1/2}$$

$$R' = [(x - \xi)^2 + (y + 2h + \eta)^2 + (z - \zeta)^2]^{1/2}$$

$$r = [(x - \xi)^2 + (z - \zeta)^2]^{1/2}$$

$$v = \frac{\sigma^2 \bar{a}}{g} = a \tanh (ah)$$

and P.V. indicates the Cauchy principle value of the integral.

An alternate series form of Green's function is also given by Wehausen and Laitone as

$$G(x, y, z; \xi, \eta, \zeta) = \frac{2\pi(v^2 - a^2)}{a^2 h - v^2 h + v} \cosh[a(h+y)] \cosh[a(h+\eta)] \cdot$$

$$[Y_0(ar) - iJ_0(ar)] \quad (24)$$

$$+ 4 \sum_{k=1}^{\infty} \frac{(\mu_k^2 - v^2)}{\mu_k^2 h - v^2 h + v} \cos[\mu_k(h+y)] \cos[\mu_k(h+\eta)] K_0(\mu_k r)$$

where J_0 and Y_0 denote, respectively, Bessel functions of the first and second kind of order zero and K_0 denotes the modified Bessel function of the second kind of order zero. The quantities μ_k are the real positive roots of the equation

$$\mu_k \tan(\mu_k h) + v = 0 \quad (25)$$

The solution to the boundary value problem now rests on the determination of the source strength function f . Taking the normal derivative of the potential u_j and applying boundary condition (18d) yields the following integral equation from which f is to be determined:

$$\frac{1}{4\pi} \iint_S f_j(\xi, \eta, \zeta) \frac{\partial G}{\partial n}(x, y, z; \xi, \eta, \zeta) ds = h_j(x, y, z) , j = 1, 2, \dots, 7 \quad (26)$$

where $\partial G/\partial n$ may be obtained by straight forward differentiation of (22) and (24).

C. NUMERICAL SOLUTION

A numerical procedure can be devised by approximating the actual contour by a profile of a finite number of facets. Proceeding in this direction, the surface of the object is partitioned into N area elements of size Δs_j where the subscript takes on values $j = 1, 2, \dots, N$. Since the source strength function f , occurring in the integrals in (20) and (25), is a continuous, well-behaved function, these integrals may be approximated by the following summations:

$$f_{nj} \alpha_{ij} = h_{ni} \quad (27)$$

$$u_{ni} = f_{ni} \beta_{ij} \quad (28)$$

where

$$\alpha_{ij} = \frac{1}{4\pi} \iint_{\Delta s_j} \frac{\partial G}{\partial n}(x_i, y_i, z_i; x_j, y_j, z_j) ds \quad (29)$$

$$\beta_{ij} = \frac{1}{4\pi} \iint_{\Delta s_j} G(x_i, y_i, z_i; x_j, y_j, z_j) ds. \quad (30)$$

In these expressions, u_{ni} denotes the potential at the i^{th} nodal point on the object associated with either the n_{th} mode

of oscillation, or scattering ($n = 7$) of the incident wave. The integrations are carried out over the finite surface area element Δs_j and f_{jn} denotes the value of f at the central point of the area element. The approximation made here is consistent in that as N approaches infinity, the approximations given in (27) and (28) approach the exact forms.

Since the matrices α , β , and h are numerically evaluated, (27) can easily be inverted by use of a standard computer subroutine to obtain the solution for f . u_n is then obtained from (29). There are, however, certain difficulties connected with the evaluation of (29) and (30) which must first be considered. Specifically for the special case when $i = j$, the $1/R$ and $\partial(1/R)/\partial n$ terms are singular as R approaches 0, and secondly in the evaluation of (29) and (30) due to the singular nature of $[1/(\mu \tanh(\mu h) - a \tanh(ah))]$ at $\mu = a$ occurring in the infinite integral in (23) and its normal derivative. These difficulties are, however, circumvented by subtracting out the singularity and carrying out its integration analytically. These details are carried out in some, yet unpublished, notes of C. J. Garrison.

D. HYDRODYNAMIC FORCES AND MOMENTS

The forces and moments caused by the dynamic fluid pressure acting upon the immersed surface of the object may be obtained from the integrals,

$$F_{ij}(t) = - (1 \text{ or } \bar{a}) \iint P_j h_i d\bar{s} \quad , \quad i, j = 1, 2, \dots, 6 \quad (31)$$

$$F_i(t) = - (1 \text{ or } \bar{a}) \iint P' h_i d\bar{s} \quad , \quad i = 1, 2, \dots, 6 \quad (32)$$

where F_i denotes the i^{th} component of wave force (or moments) and F_{ij} denotes the i^{th} component of forces arising from the j^{th} component of body motion. The coefficient 1.0 is used for the case of a force ($i = 1, 2, 3$) whereas \bar{a} is used when F denotes a moment ($i = 4, 5, 6$).

For purposes of presentation of the numerical results, dimensionless force coefficients are defined as

$$C_i = \frac{F_{i\max}}{\rho g \bar{a}^3 \eta} e^{i\delta_i} \quad , \quad i = 1, 2, 3 \quad (33)$$

and

$$C_{ij} = \frac{F_{i\max}}{\rho g \bar{a}^4 X_j} e^{i\delta_{ij}} = -M_{ij} - iN_{ij}, \quad \begin{matrix} i = 1, 2, 3 \\ j = 1, 2, \dots, 6. \end{matrix} \quad (34)$$

The corresponding expressions for the moment coefficient are

$$C_i = \frac{F_{i\max}}{\rho g \bar{a}^4 \eta} e^{i\delta_i} \quad , \quad i = 4, 5, 6 \quad (35)$$

and

$$C_{ij} = \frac{F_{i\max}}{\rho g \bar{a}^4 X_j} e^{i\delta_{ij}} = -M_{ij} - iN_{ij}, \quad \begin{matrix} i = 4, 5, 6 \\ j = 1, 2, \dots, 6. \end{matrix} \quad (36)$$

The complex coefficients C_i relate to the i^{th} component of wave force (or moment) coefficient while C_{ij} denotes the i^{th} component of force (or moment) coefficient associated with the j^{th} component of oscillation of the object. The phase

shift angles δ_i and δ_{ij} relate the phase of the force to the crest of the incident wave and displacement of the body, respectively. The real and imaginary parts of the dimensionless force coefficients, M_{ij} and N_{ij} , are called the added mass and the damping coefficients, respectively.

Using (31) and (32) in conjunction with (16) and (17) and the definitions (33-36), the force coefficients may be written in dimensionless form as

$$C_i = \iint_s [au_7(x,y,z) - \frac{\cosh[a(h+y)]}{\cosh(ah)}] h_i(x,y,z)ds, \quad i = 1,2,\dots,6 \quad (37)$$

and

$$C_{ij} = \iint_s u_j(x,y,z)h_i(x,y,z)ds, \quad i, j = 1, 2, \dots, 6. \quad (38)$$

Once $u_j(x,y,z)$ is obtained from (28), the coefficients can be obtained from (37) and (38) by numerical quadrature.

E. HASKIND'S RELATIONS AND ENERGY CHECK

Although it may be presupposed that the numerical solution outlined here will converge upon increasing the number of partitions, modern computers are still limited by storage capacity and computer time is expensive. In view of this, it is necessary to keep the partition size as large, i.e., the number of partitions as small, as accuracy considerations permit. The determination of the effect of the partition size on accuracy becomes, therefore, an important consideration in order that practical limits may be established. One

available method is the comparison of the numerical results with analytical results where closed form solutions exist. This approach, however, is limited to a few simple shapes; for more general configurations no such check, of course, exists.

A method which is valid for checking the soundness of the numerical results of any shape is the use of the so-called Haskind's relations as well as an energy balance, both of which are developed in the Appendix. The former is used to verify the solution for the diffraction problem and the latter the solution of the radiation problem. Using the asymptotic form of Green's function as given in (24) in conjunction with (20) the following relationship for the damping coefficient is so obtained

$$N_{ii} = \frac{1}{2\rho} \left[\frac{a^2 - v^2}{a_h^2 - v_h^2 + v} \right] \int_0^\pi \left| \iint_S f_i(\xi, \eta, \zeta) \cosh[a(h+\eta)] e^{-i a \rho_1 \cos(\beta - \theta)} ds \right|^2 d\theta \quad (39)$$

where $\rho_1 = (\xi^2 + \zeta^2)^{1/2}$ and $\beta = \arctan(\zeta/\xi)$. This relates the damping coefficient to the far field behavior of the solution. It is in effect, an energy balance between the energy required to oscillate the body and the energy transmitted across some control surface a large distance from the body.

A relationship somewhat similar to (39), known as Haskind's relations, may be obtained for the wave force (or moment)

coefficient and relates the wave produced at infinity by the body oscillating in the j^{th} mode to the j^{th} component of wave force as

$$C_j = \frac{1}{\cosh(ah)} \iint_S f_j(\xi, \eta, \zeta) \cosh[a(h+\eta)] e^{-ia\rho_1 \cos(\beta-\pi)} ds. \quad (40)$$

This result represents the Haskind's relation for finite depth as given by Seetharama Roa [4].

Equations (39) and (40) represent relations for the damping and wave force (or moment) coefficient based on the behavior of the far field solution. A comparison of these results with N_{ij} and C_j obtained from an integration of the pressure over the immersed surface, i.e., as obtained from (37) and (38), provides a convenient and valuable self-check on the accuracy of the numerical results. These results are not limited to special configurations and may be applied to arbitrary shapes. Equation (40) is, however, limited to symmetry with respect to the x-y plane, a condition which is generally satisfied by practical shapes.

III. COMPUTER PROGRAM

In order to feasibly utilize the method described in section D of THEORETICAL CONSIDERATIONS, a computer program was developed to carry out the indicated calculations. Although accuracy was a controlling factor, as it should be, the primary requirement was to hold the computer run time to a reasonable value. To achieve this, every advantage was taken to employ the symmetry in the equations and to eliminate redundant computations by generating certain constants and matrices.

The program consists of several subroutines, each solving a specific part of the problem. This allowed the development of the program to be simplified and the use of it was made easier in that only a small main program was required to execute the program. Subroutine GEODAT reads the input geometrical data, generates the matrix h as defined in (19), and, in conjunction with GCOEFF, calculates certain geometrical parameters. GARRIS, the primary subroutine, then generates the α and β matrices by calling either of two subroutines. The first (GREEN) calculates G and $\partial G / \partial n$ based on the integral form given in (22) and (23) whereas the second (GREENS) makes evaluations on the basis of the alternate series formulations given in (24). For elements of the α and β matrices corresponding to small values of (ar) GREEN is utilized, while for large values of (ar) GREENS is used. With the exception of the diagonal elements, the majority of the elements of α and

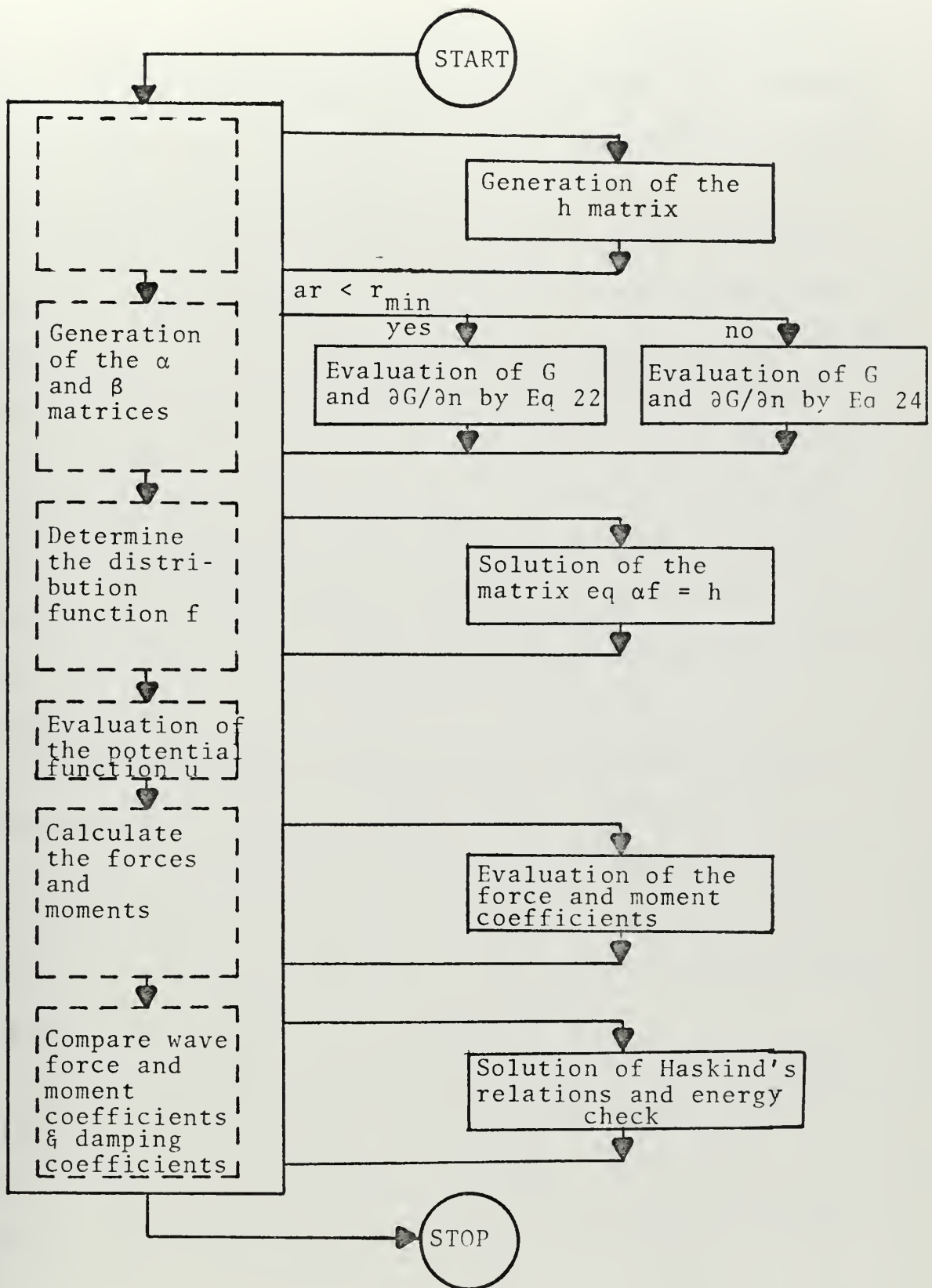


Figure 2: Program Flow Chart

β are calculated by the latter subroutine. This situation proved to be most fortunate because the series form converges rather rapidly and, consequently, requires much less computer time than the integral form.

In order to check the validity of the two subroutines, values of G were computed. A comparison between GREEN and GREENS, Figs. 3, 4, 5, for constant a and decreasing r , shows that at small values of a , the two methods give similar results whereas at intermediate values of a , the GREEN solution becomes very erratic at larger values of r . At high values of a , however, the two subroutines render similar solutions despite the higher frequency of oscillation. This stems from the fact that the amplitude of oscillation decays extremely fast.

Subroutine COMAT then determines the source strength function f by solving the complex matrix equation (27). Once the matrix f has been generated, the potential function u is calculated by (28). The pressure at points on the immersed surface as well as the resulting forces and moments are then determined in subroutine FORCES.

Finally, the Haskind's relations and the energy check are employed to calculate the wave force and moment coefficients and the damping coefficients in COCHCK. Here also, a comparison is made between these values and those found in FORCES.

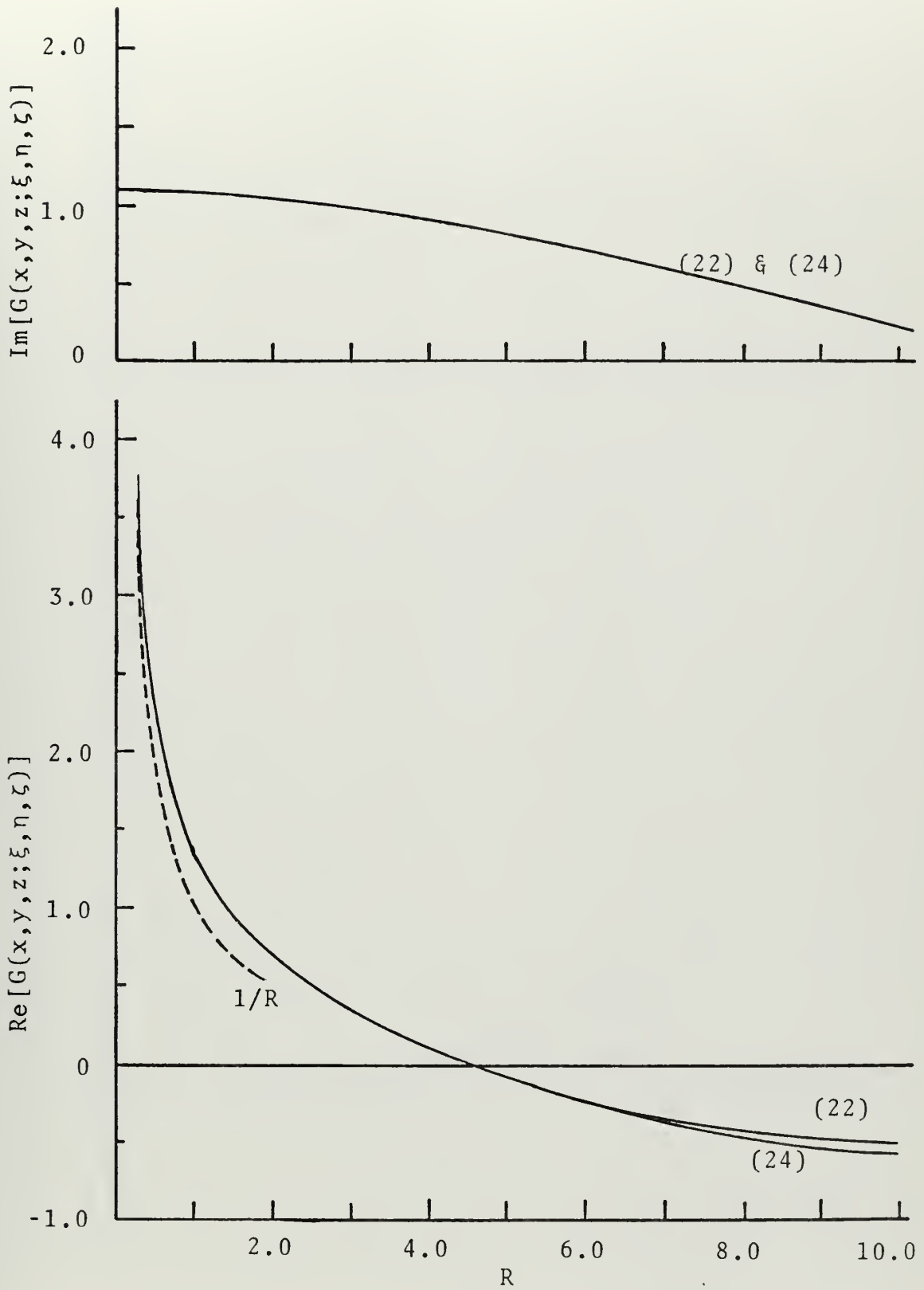


Figure 3: Comparison of Equations (22) and (24); $a = 0.2$

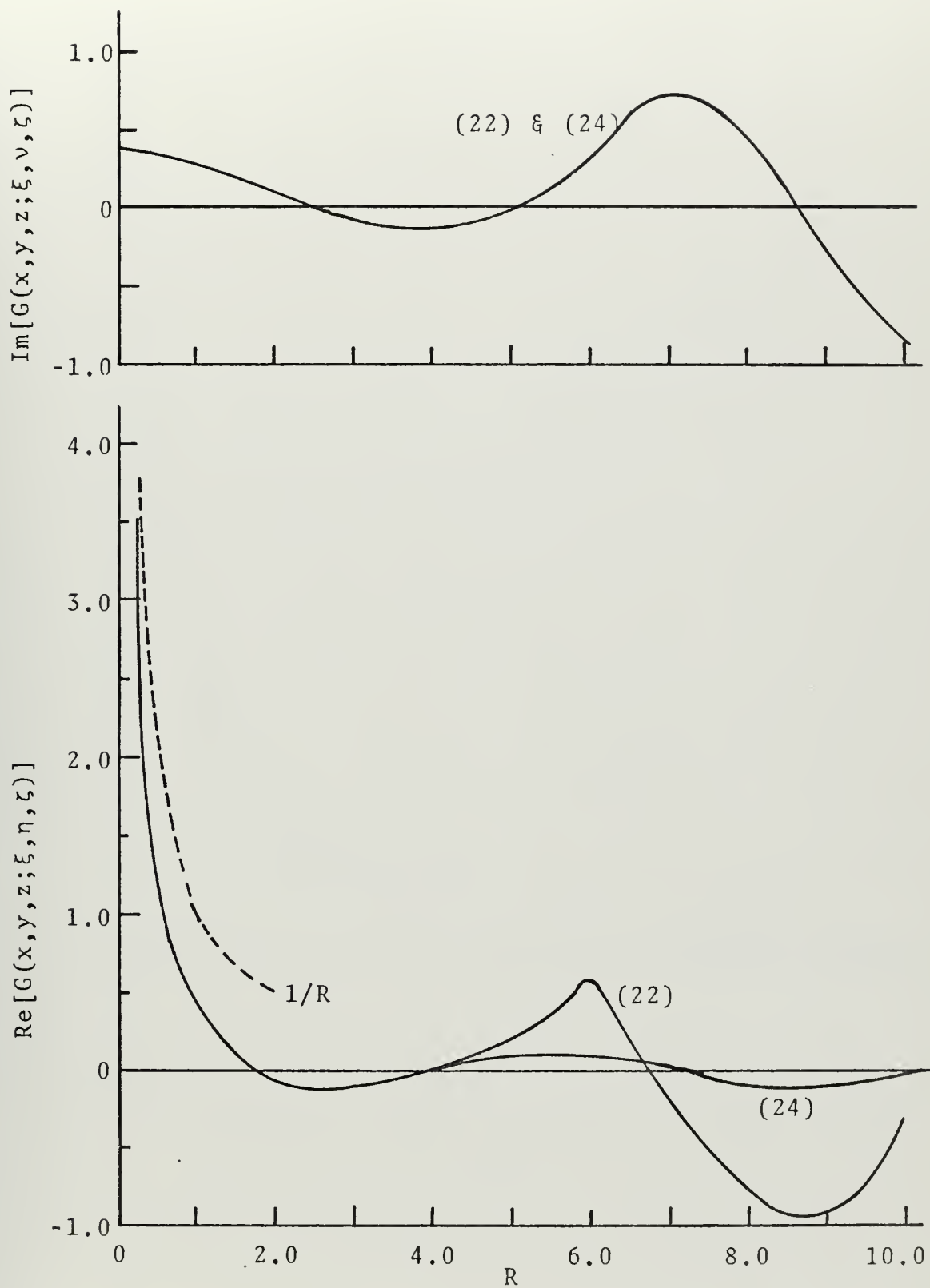


Figure 4: Comparison of Equations (22) and (24); $a = 1.0$

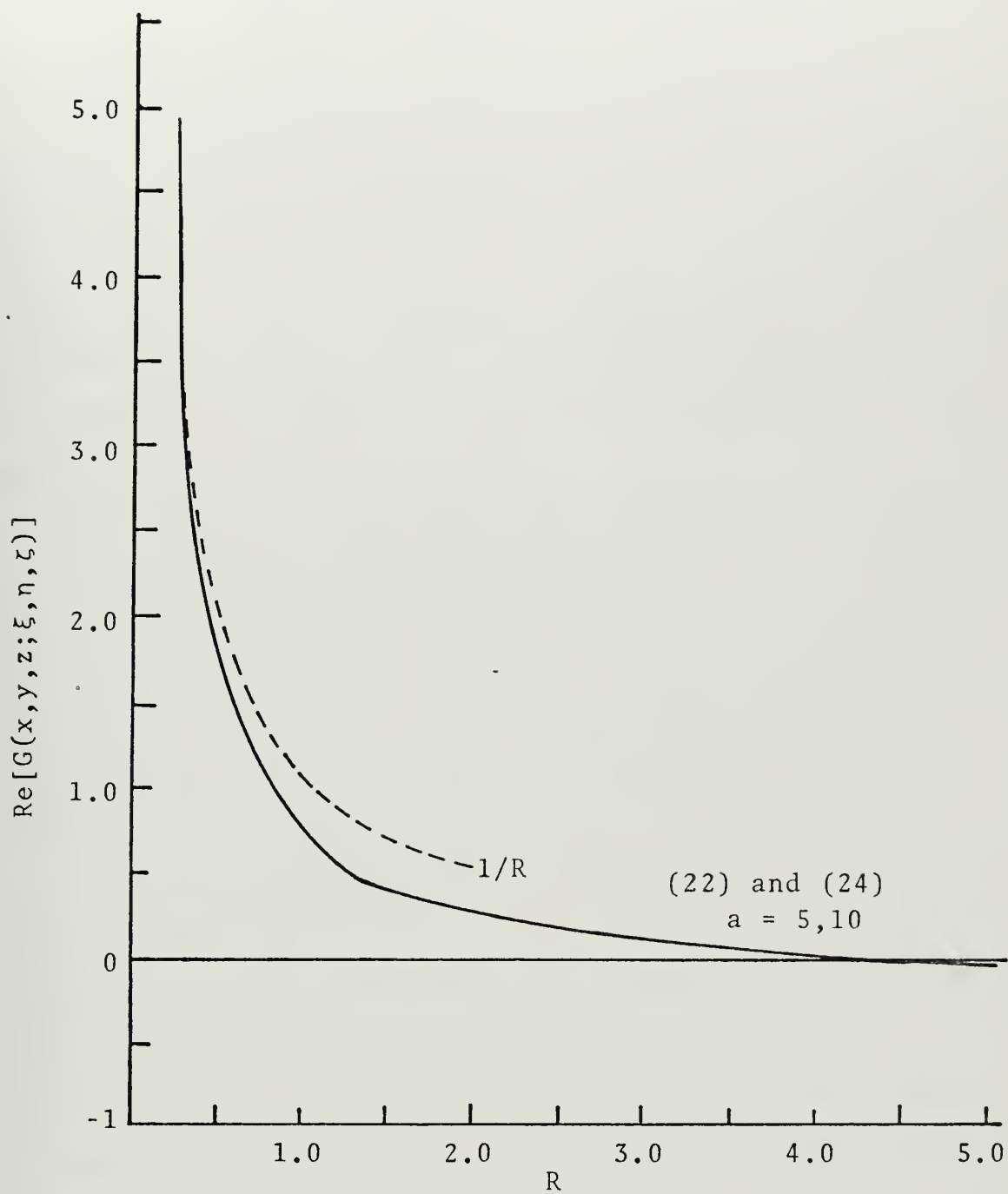


Figure 5: Comparison of Equations (22) and (24) for Large a .

IV. DISCUSSION OF RESULTS

A. VERTICAL CYLINDER

In order to study the accuracy of the computer program, numerical results were generated for both the wave force problem and the problem involved in the oscillation of the object in otherwise still water. Simple geometric shapes, including vertical circular cylinders and submerged spheres, were studied and compared with closed form solutions where they exist.

As indicated in Section II, the accuracy of the numerical results is dependent on the size of the grid. Garrison [Ref. 5], for one, found that the fineness of the grid size, N , must be increased as a increases. This results from the fact that the kernels of the integral equations oscillate rapidly as the parameter a increases.

A series of computer runs was made for a vertical circular cylinder resting on the bottom and piercing the free surface. Two runs consisting of cylinders with grid sizes $N = 120$ and $N = 252$ were made for a relative depth of $h = 2.0$ in order to determine the effect of the grid size. Another was made with $N = 120$ and $h = 6.0$ to determine the effect of depth. A fourth run was made with $N = 240$ and $h = 4.0$, but this time the grid was divided into two sizes. The bottom half of the cylinder had $N = 96$ with an element aspect ratio (width/height) of 0.525 whereas the top half had $N = 144$ and an aspect ratio of 0.785.

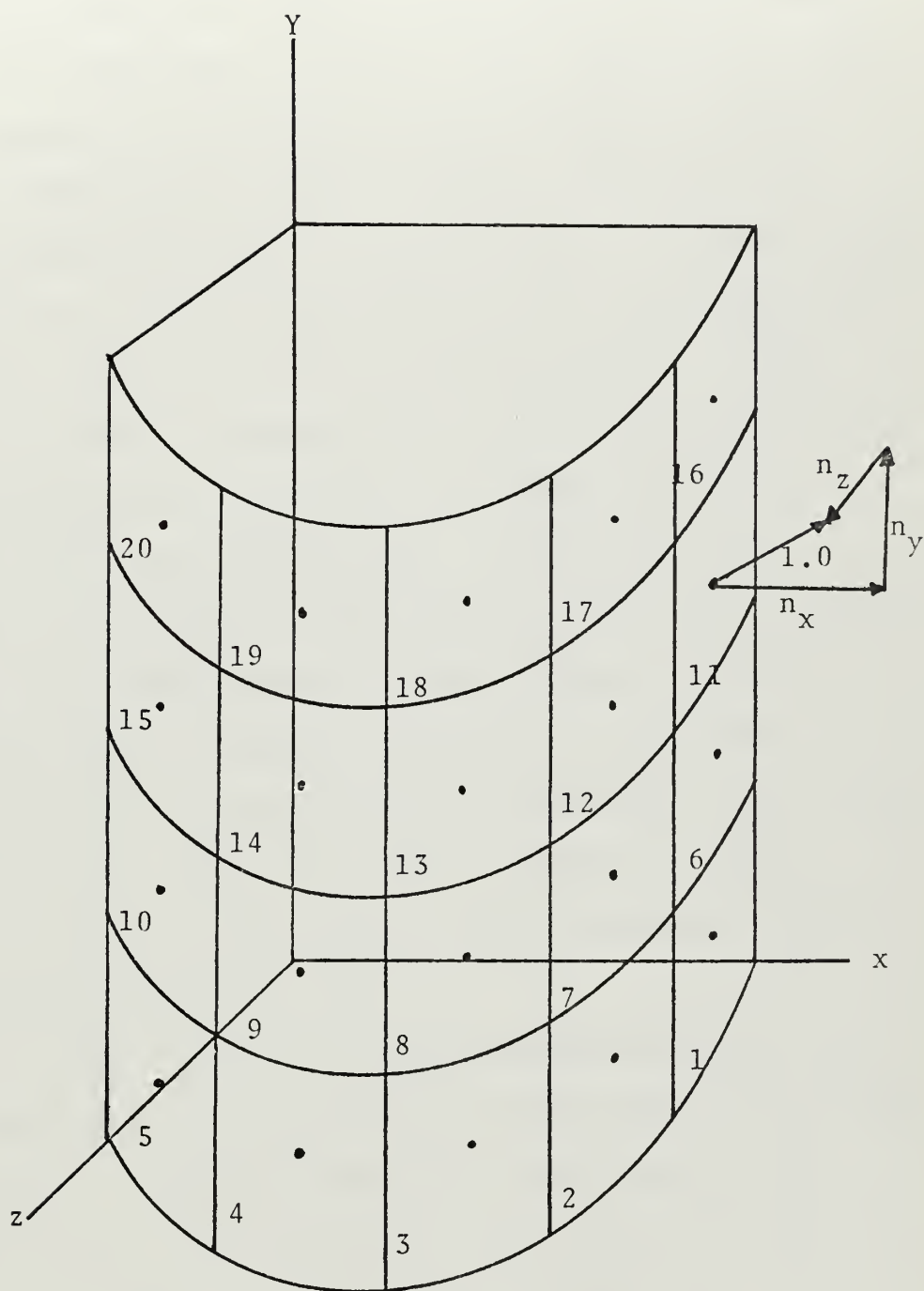


Figure 6: Definition Sketch

Within the range of practicality of a , $a = 0$ to $a = 3.0$, the numerical results for the horizontal wave force coefficient and the coefficient of moment about a bottom line axis compared favorably with the closed form solution given by MacCamy and Fuchs [Ref 6], Figs. 7 and 8. These results show that within this range of the parameter a , there is such a small deviation in the values obtained for the different grid sizes that the two curves are superimposed. As the frequency is increased, however, it was found that deviation from the closed form results increased more rapidly for the coarser grid than the finer one. It is also noteworthy that the magnitude of the moment coefficient relative to the wave force coefficient is small at low frequencies and increases as the frequency increases. This result is as expected since at small values of wavelength, wave action is concentrated near the free surface whereas at large values of wavelength, wave action is felt at deeper depths, thus decreasing the moment arm.

Figures 9 and 10 represent the hydrodynamic force and moment coefficients associated with the cylinder oscillating in still water. These show that for zero frequency, the force coefficient, C_{11} , approaches approximately 2π and 4π for the $h = 2.0$ and $h = 4.0$ cylinder, respectively. At $h = 6.0$ a value of approximately 6π was obtained. When this is converted to an added mass coefficient the result is 1.0. This is as expected since at zero frequency the free surface acts as a rigid boundary and the flow corresponds to

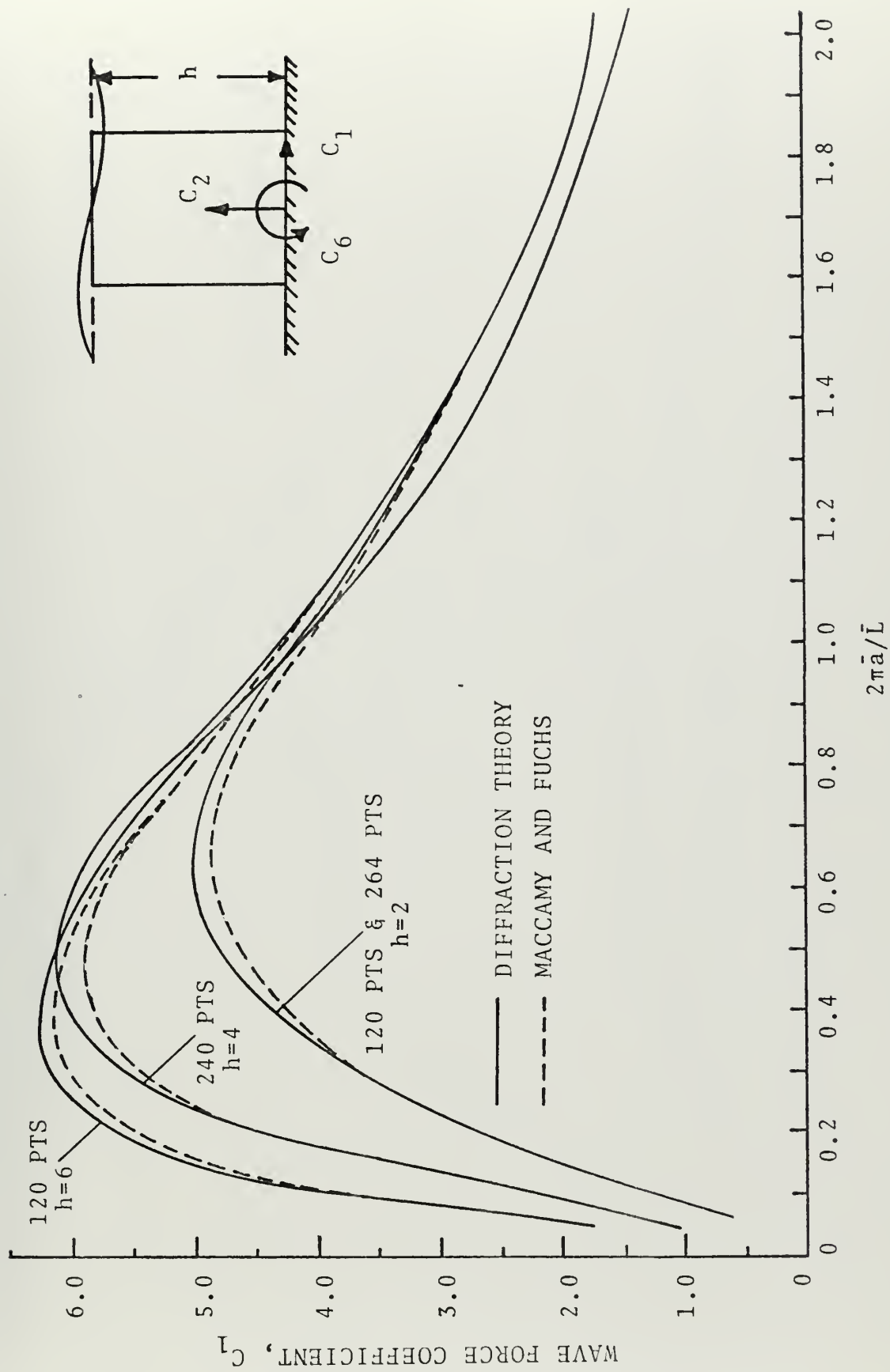


Figure 7: HORIZONTAL WAVE FORCE COEFFICIENT FOR A VERTICAL CIRCULAR CYLINDER

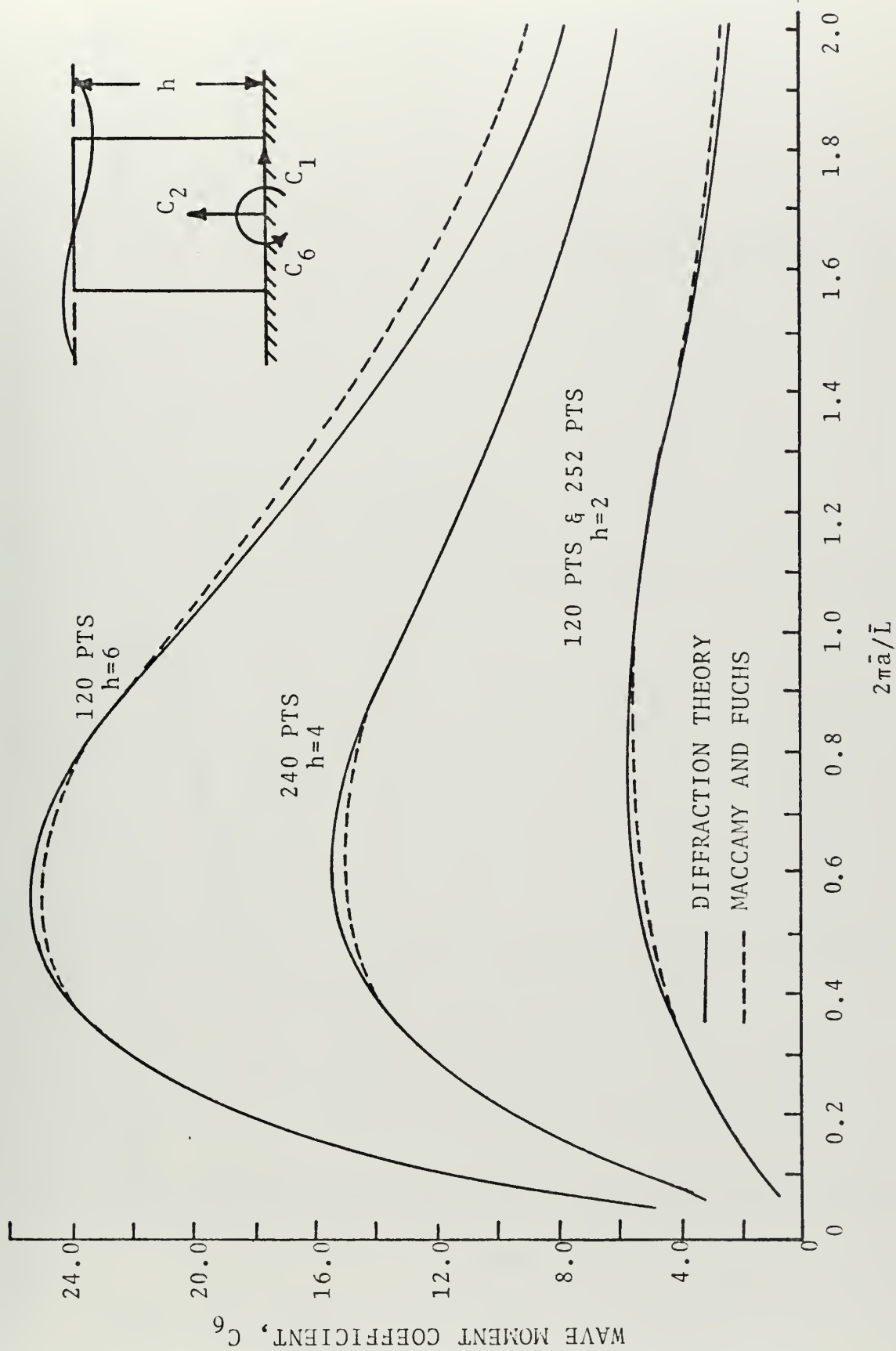


Figure 8: HORIZONTAL WAVE MOMENT COEFFICIENT FOR A VERTICAL CIRCULAR CYLINDER

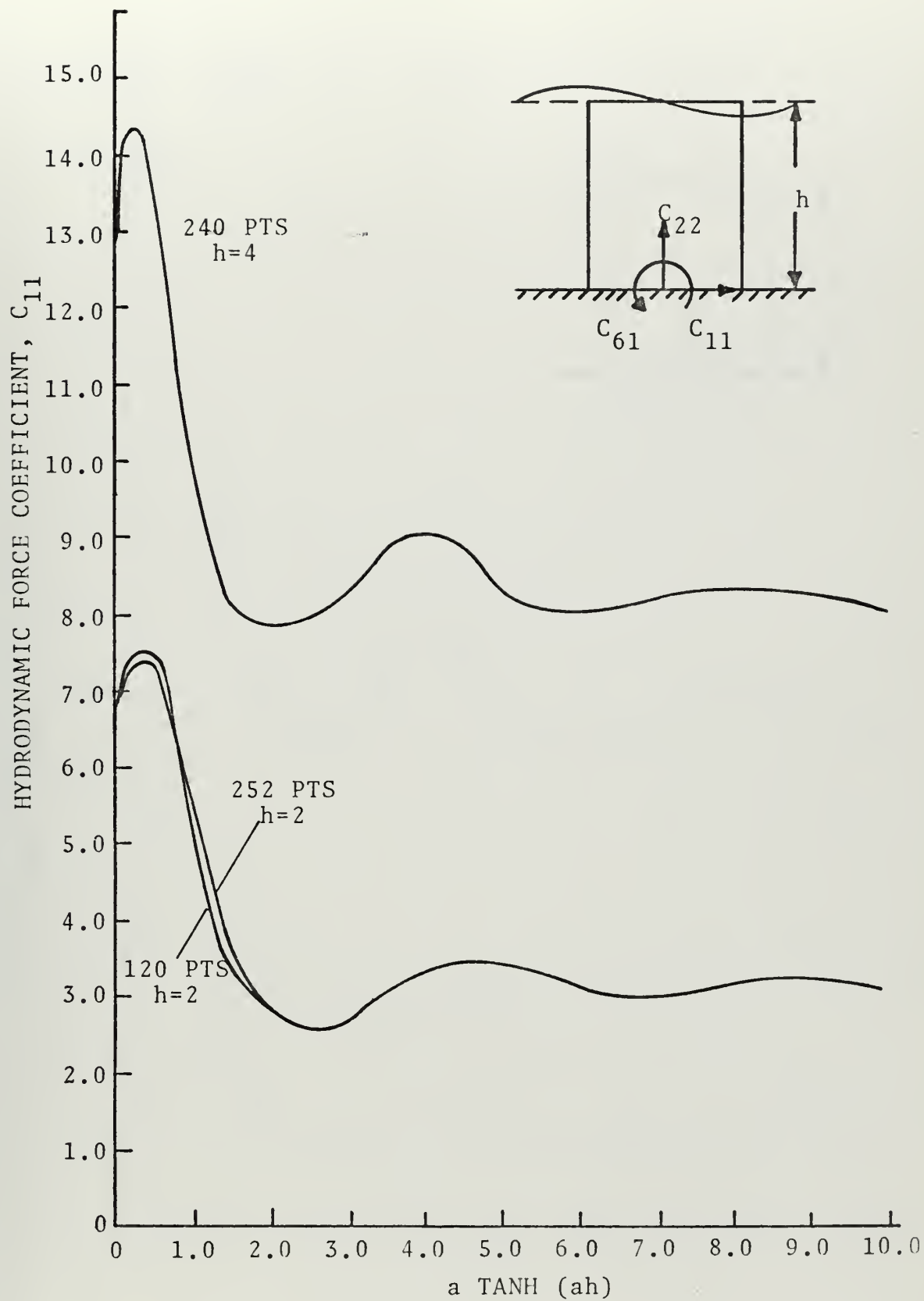


Figure 9: HYDRODYNAMIC FORCE COEFFICIENT FOR A VERTICAL CIRCULAR CYLINDER

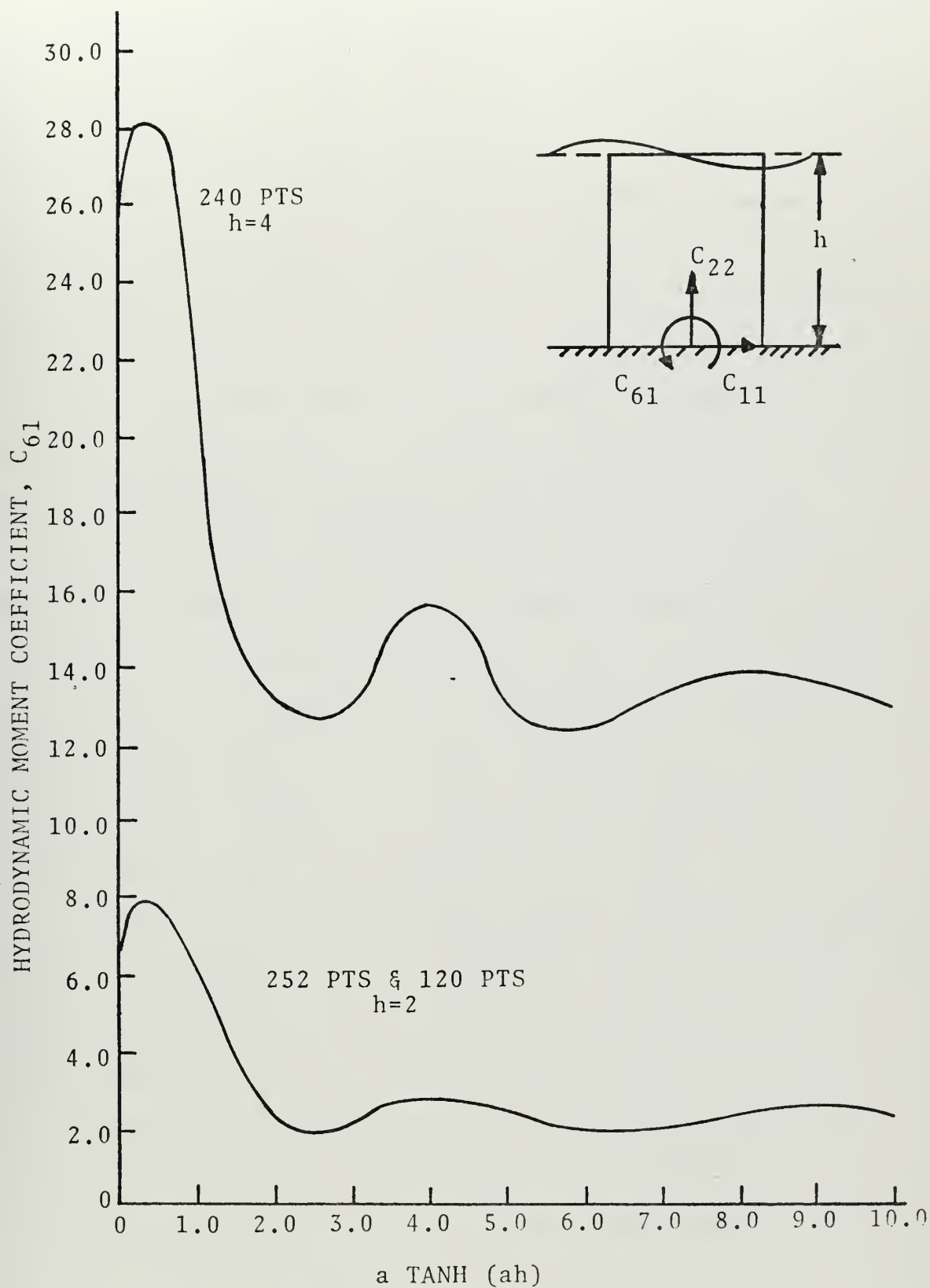


Figure 10: HYDRODYNAMIC MOMENT COEFFICIENT FOR A VERTICAL CIRCULAR CYLINDER

two-dimensional flow past a circular cylinder. The classical value for the added mass coefficient in this case is 1.0.

B. SPHEROID

A series of runs for varying a was made for a half submerged sphere. One consisted of a grid size of 200 points with the relative depth $h = 5.0$ and the others were made with a grid size of 264 points and $h = 5.0$ and $h = 10.0$. Havelock [Ref. 7] determined the added mass and damping coefficients for a floating, heaving sphere. His results were later confirmed by Kim [Ref. 8] who also obtained such values for floating, surging (or swaying) spheroids. Although the results found by Havelock and Kim were for infinite depth, the values found in this study for $h = 5.0$ and 10.0 , Figs. 11-16, compare quite favorably. There is apparently little depth effect beyond $h = 5.0$ except at small values of a where it is noted the curves corresponding to $h = 5.0$ and $h = 10.0$ differ.

Kim [Ref. 9] also determined the horizontal and vertical wave force coefficients as did Milgram and Halkyard [Ref. 10]. Comparison of these values with those calculated in this study, Figs. 15 and 16, show good agreement with the former, but some difference was noted with the latter, especially for the vertical force coefficient where the value of Milgram and Halkyard was almost three times greater at $a = 2.0$. It would appear the Milgram and Halkyard results are in error.

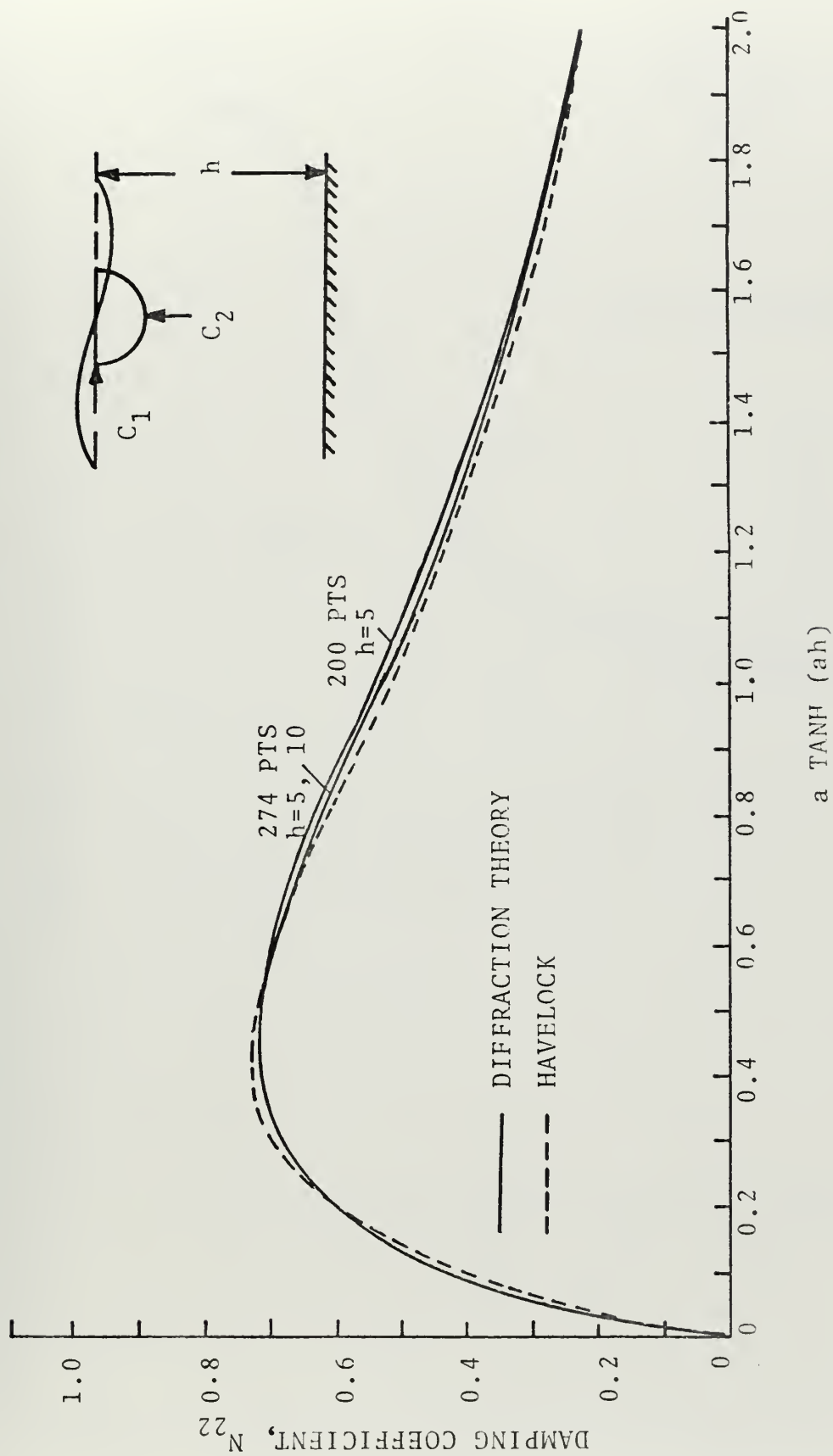


Figure 11: COEFFICIENT OF DAMPING FOR A HEAVING SPHERE

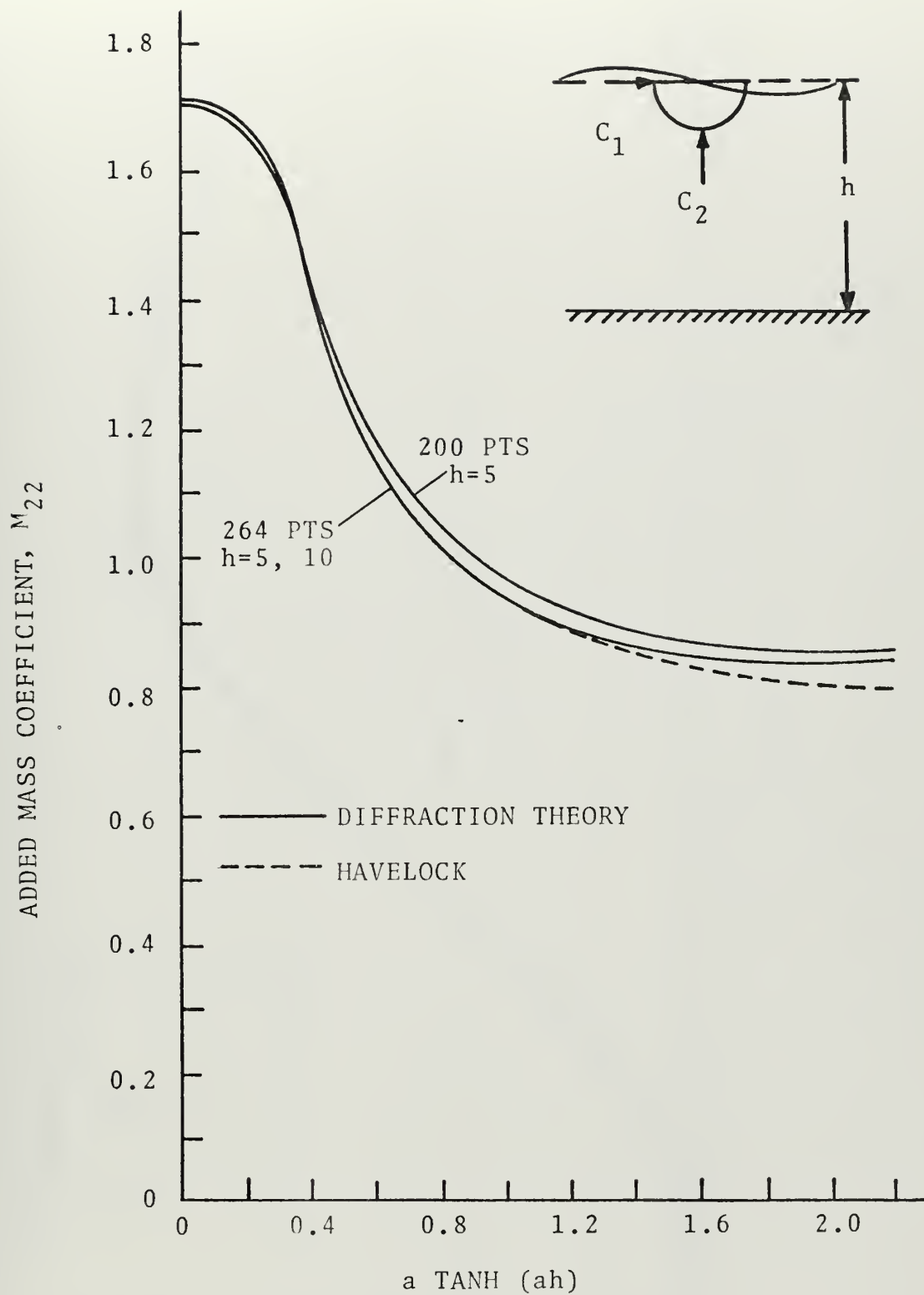


Figure 12: COEFFICIENT OF ADDED MASS FOR A HEAVING SPHERE

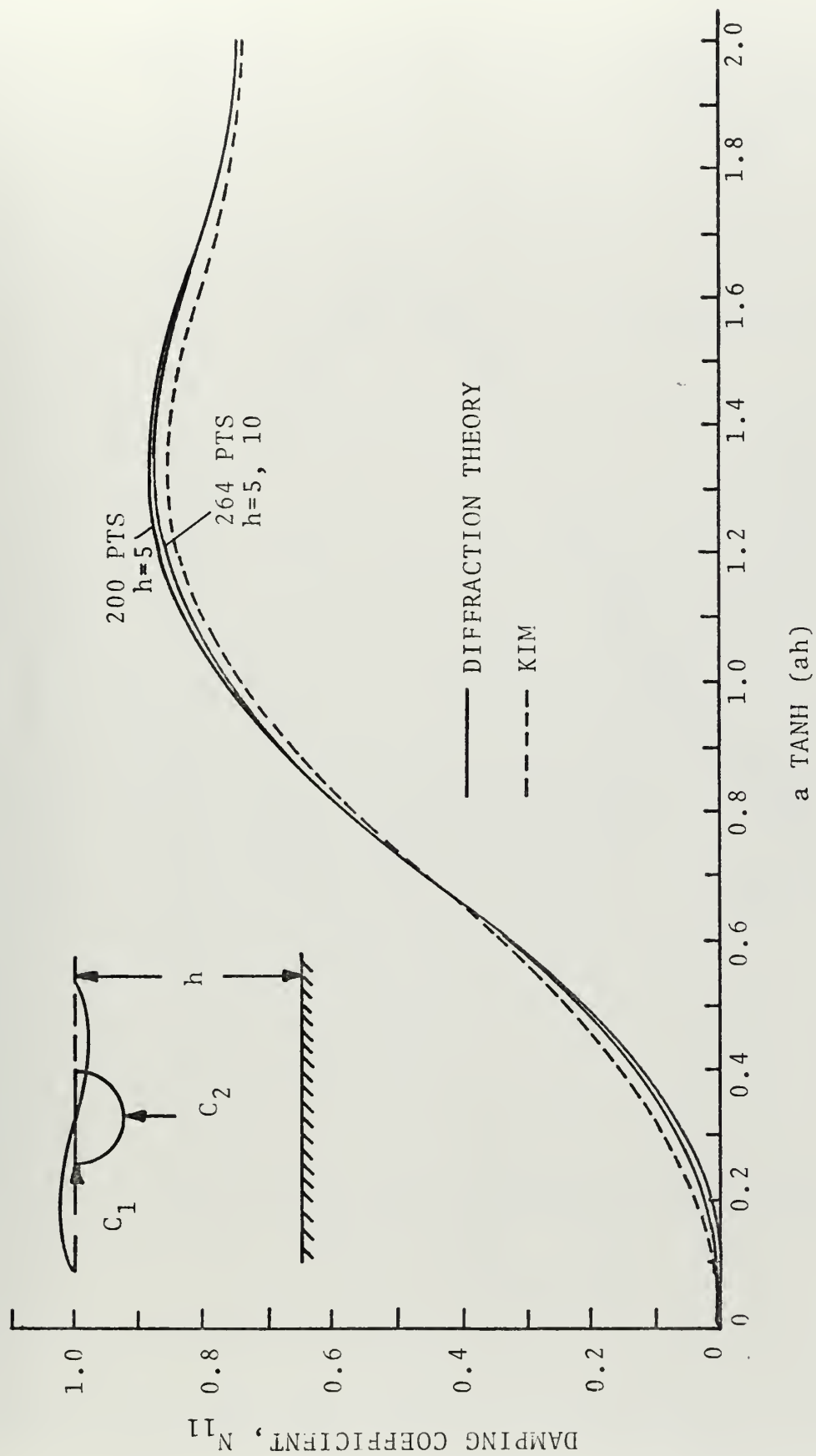


Figure 13: COEFFICIENT OF DAMPING FOR A SURGING SPHERE

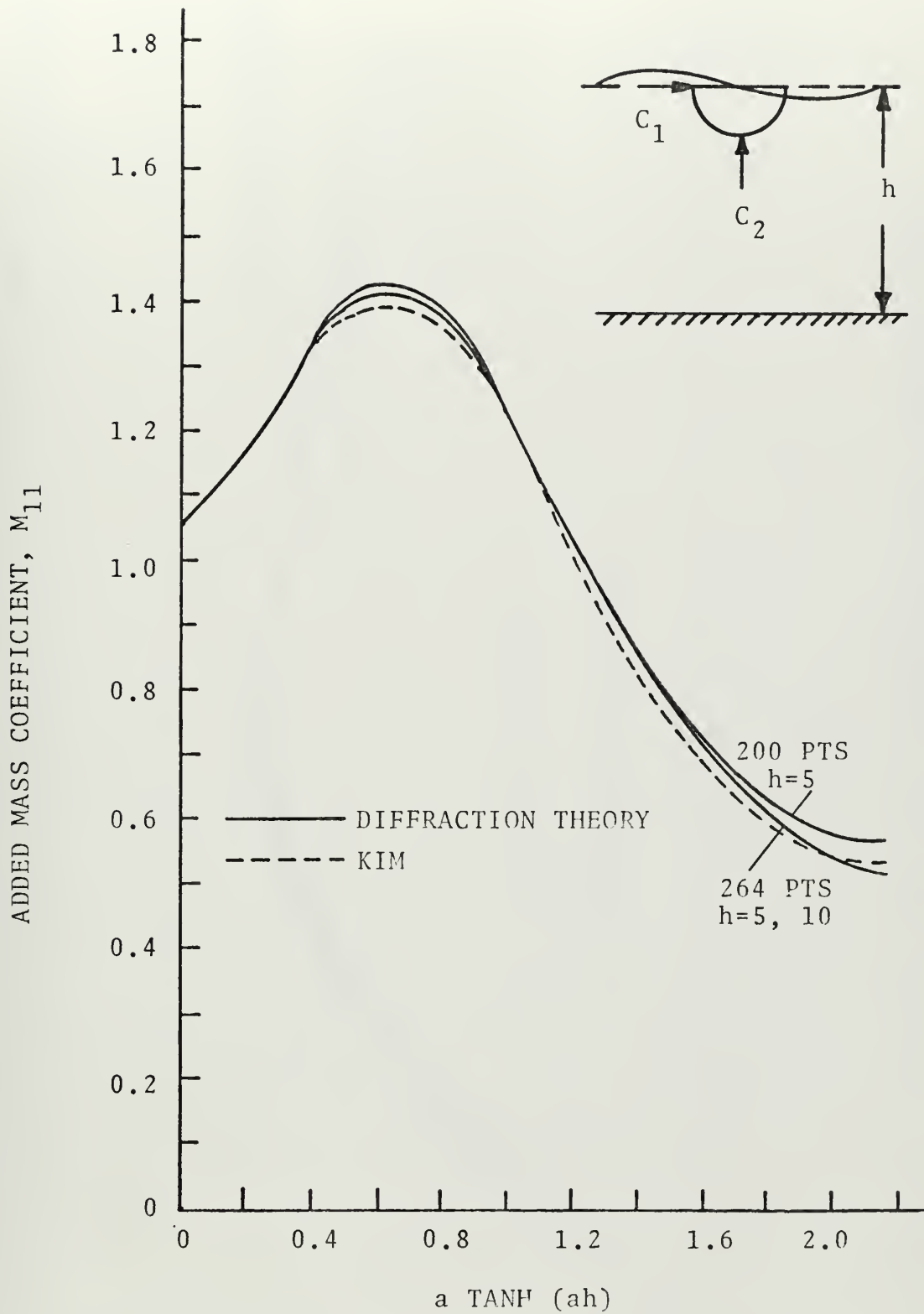


Figure 14: ADDED MASS COEFFICIENT IN SURGE FOR A FLOATING SPHERE

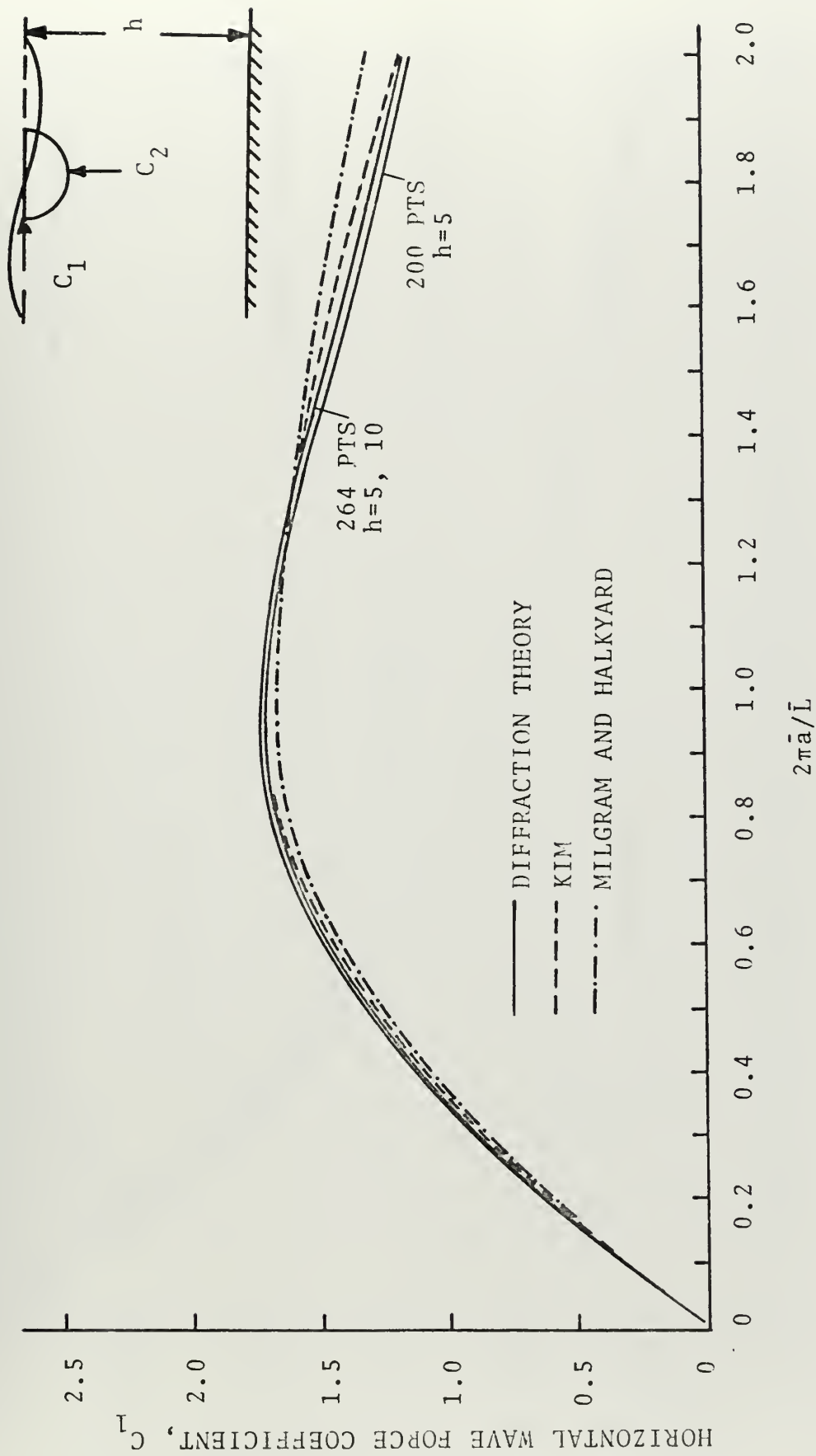


Figure 15: HORIZONTAL WAVE FORCE COEFFICIENT FOR A FLOATING SPHERE

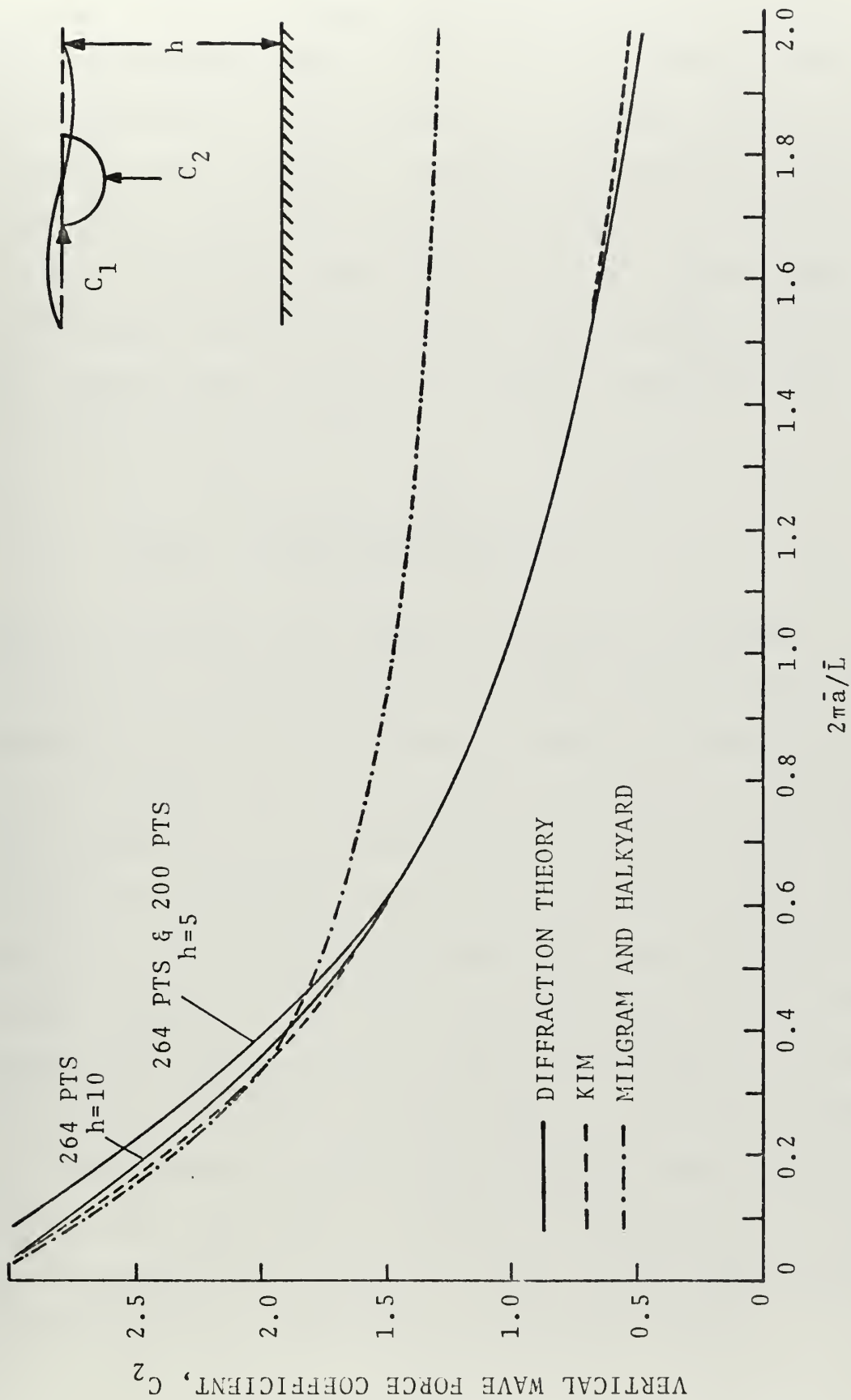


Figure 16: VERTICAL WAVE FORCE COEFFICIENT FOR A FLOATING SPHERE

For a fully submerged spheroid there were only two available checks known. One is that the value of the added mass coefficient for a sphere in an infinite fluid is 0.5. Figure 18 shows that for the numerical procedure used in this study a value of 0.51 was obtained for a relative depth of 5.0. The second test involves the use of Haskind's relations which relates the vertical force on an object fixed in a monochromatic wave train with the heave damping coefficient N_{22} such that

$$N_{22}^* = \frac{a}{2} \frac{\sinh(2ah)}{2ah + \sinh(2ah)} C_2^2 \quad (41)$$

where N_{22}^* denotes the damping coefficient in heave. A comparison of the damping coefficient found in this study with that using (41) is shown in Table 1. Using the results of the diffraction theory as the standard, the percentage deviations from it for the Haskind's relations are also shown. The comparison shows that for values of a greater than 0.5, all of the results obtained were within 4% of the taken standard. For values of a less than 0.5, the differences were considerable and this was believed to be due to the low value of the relative depth h . A similar comparison was made for the 264 point floating sphere using $h = 10.0$. The results are shown in Table 2. Since the present results satisfy Haskind's relations, it may be concluded the Milgram and Halkyard's results are definitely in error.

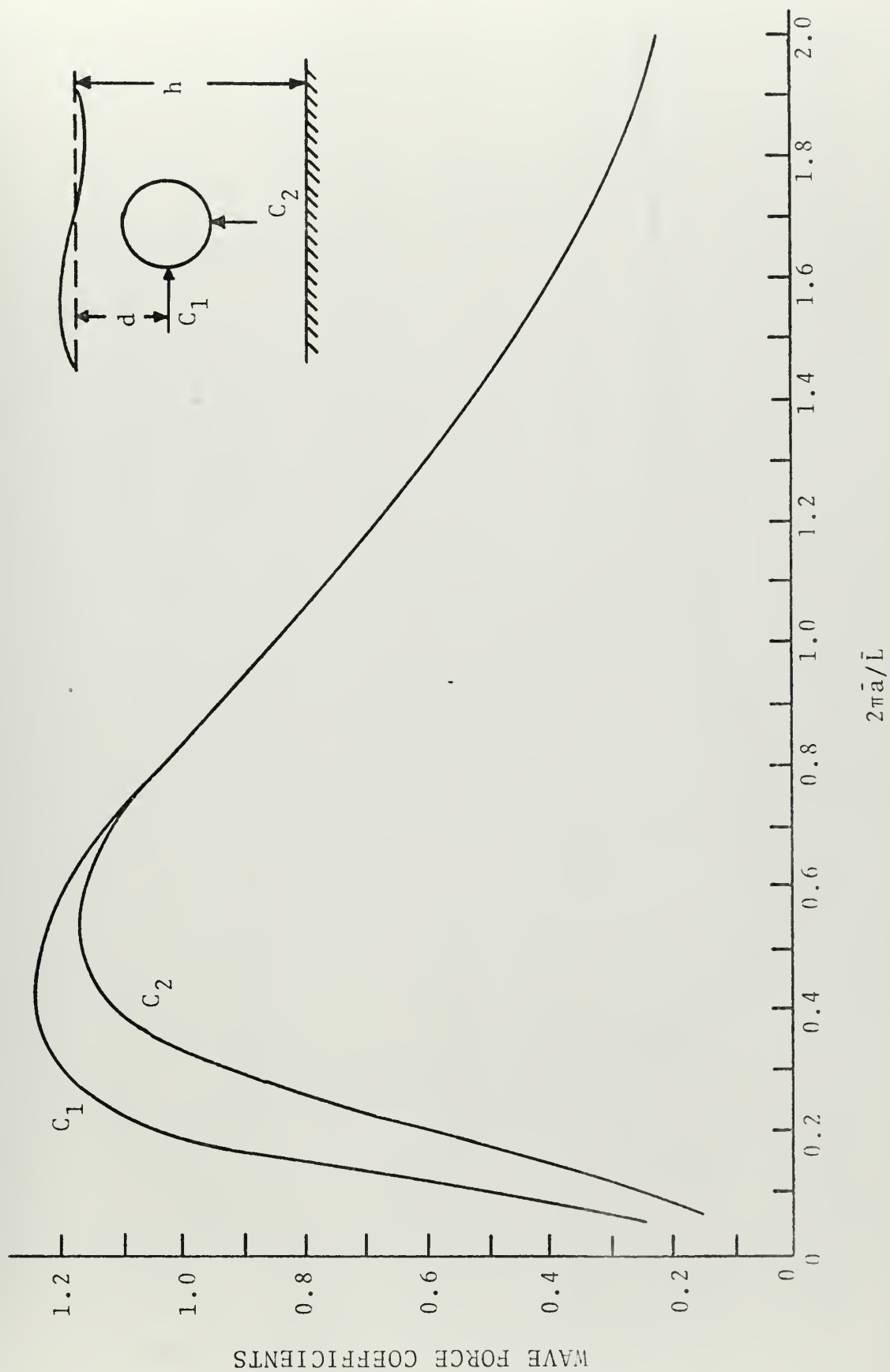
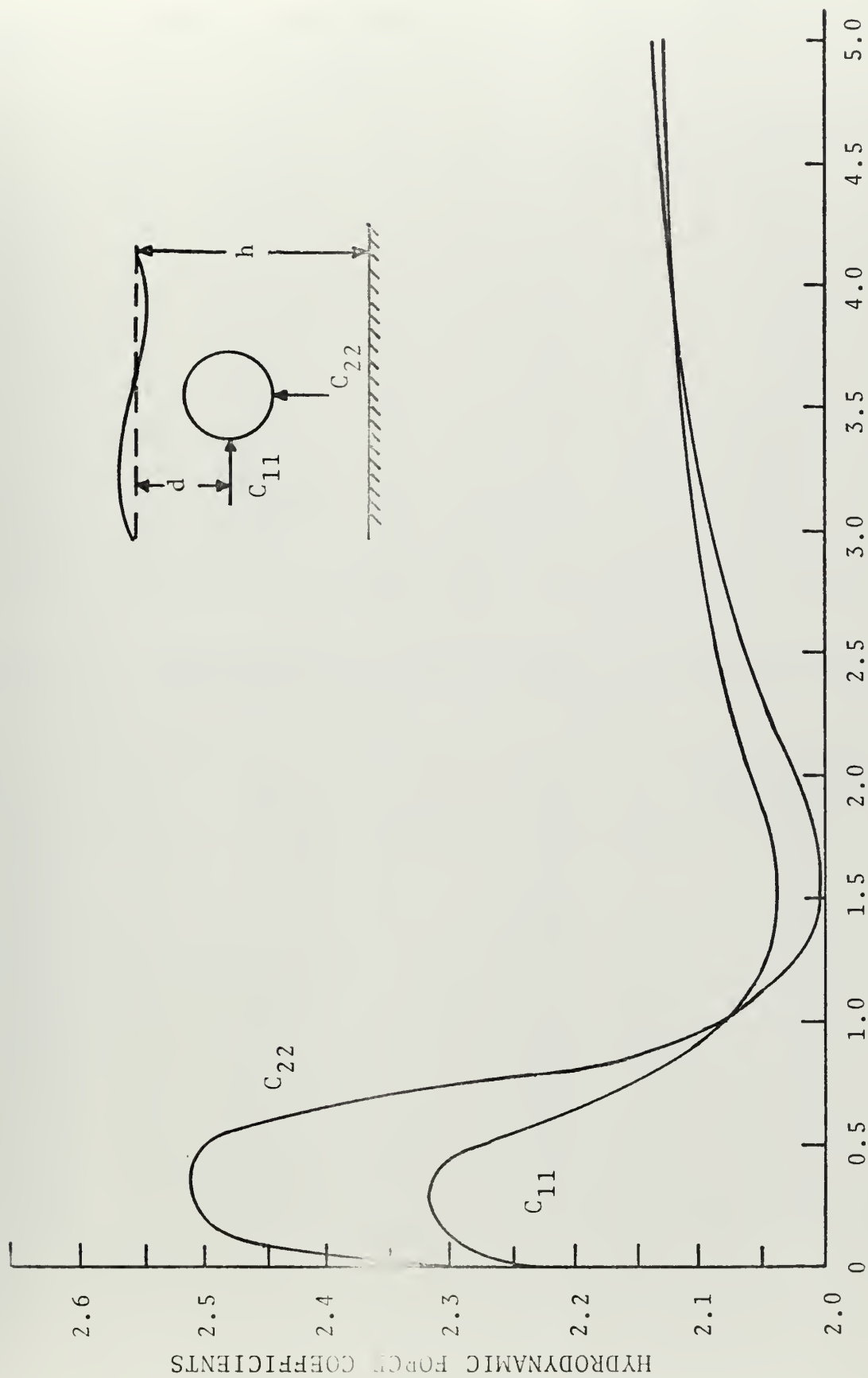


Figure 17: WAVE FORCE COEFFICIENTS FOR A SUBMERGED SPHERE; 200 PTS, $h=5$, $d=2$



a $\tanh(ah)$

Figure 18: HYDRODYNAMIC FORCE COEFFICIENTS FOR A SUBMERGED SPHERE; 200 PTS, $h=5$, $d=2$

Table 1: Damping Coefficient in Heave for a Submerged Sphere

$N = 200$

$h = 5.0$

a	N_{22}	N_{22}^*	% deviation
0.20	0.0267	0.0199	25.46
0.30	0.1033	0.0914	11.52
0.50	0.3382	0.3252	3.84
0.80	0.4433	0.4329	2.34
1.00	0.3745	0.3698	1.25
1.50	0.1610	0.1589	1.30
2.00	0.0514	0.0515	-0.19
3.00	0.0033	0.0034	-3.03
4.00	0.0002	0.0002	0.0
5.00	0.0	0.0	0.0

Table 2: Damping Coefficient in Heave for a Floating Sphere

$N = 264$

$h = 10.0$

a	N_{22}	N_{22}^*	% deviation
0.20	0.5650	0.5278	6.58
0.40	0.7071	0.6919	2.15
0.60	0.6968	0.6920	0.69
0.80	0.6250	0.6071	2.86
1.00	0.5356	0.5202	2.87
1.20	0.4525	0.4388	3.02
1.40	0.3799	0.3679	3.15
1.60	0.3176	0.3075	3.18
1.80	0.2654	0.2555	3.73
2.00	0.2211	0.2304	-4.20

C. HASKIND'S RELATIONS AND ENERGY CHECK

As previously indicated, important checks on the numerical technique and the final results can be made by application of Haskind's relations and the energy check which are developed in the Appendix. These checks were applied to all computer runs made and the percent difference, using the surface integration of the pressure results as the standard, is plotted in Figs. 19 and 20.

In general, it was noted that dependence of the results on the grid size, N , is much greater for the forces obtained by a surface integration of the pressure when calculated by use of Haskind's relations. It can be seen from Figs. 19 and 20 that as frequency decreases, the percent deviation decreases. At large values of a the error becomes quite large. The effect of decreasing the grid size or increasing the depth is also clearly shown. For the 120 point grid the errors are much larger than for the 240 point grid in the case of the $h = 2.0$ circular cylinder. Similarly the errors for the 120 point grid are much smaller for $h = 6.0$ than for $h = 2.0$.

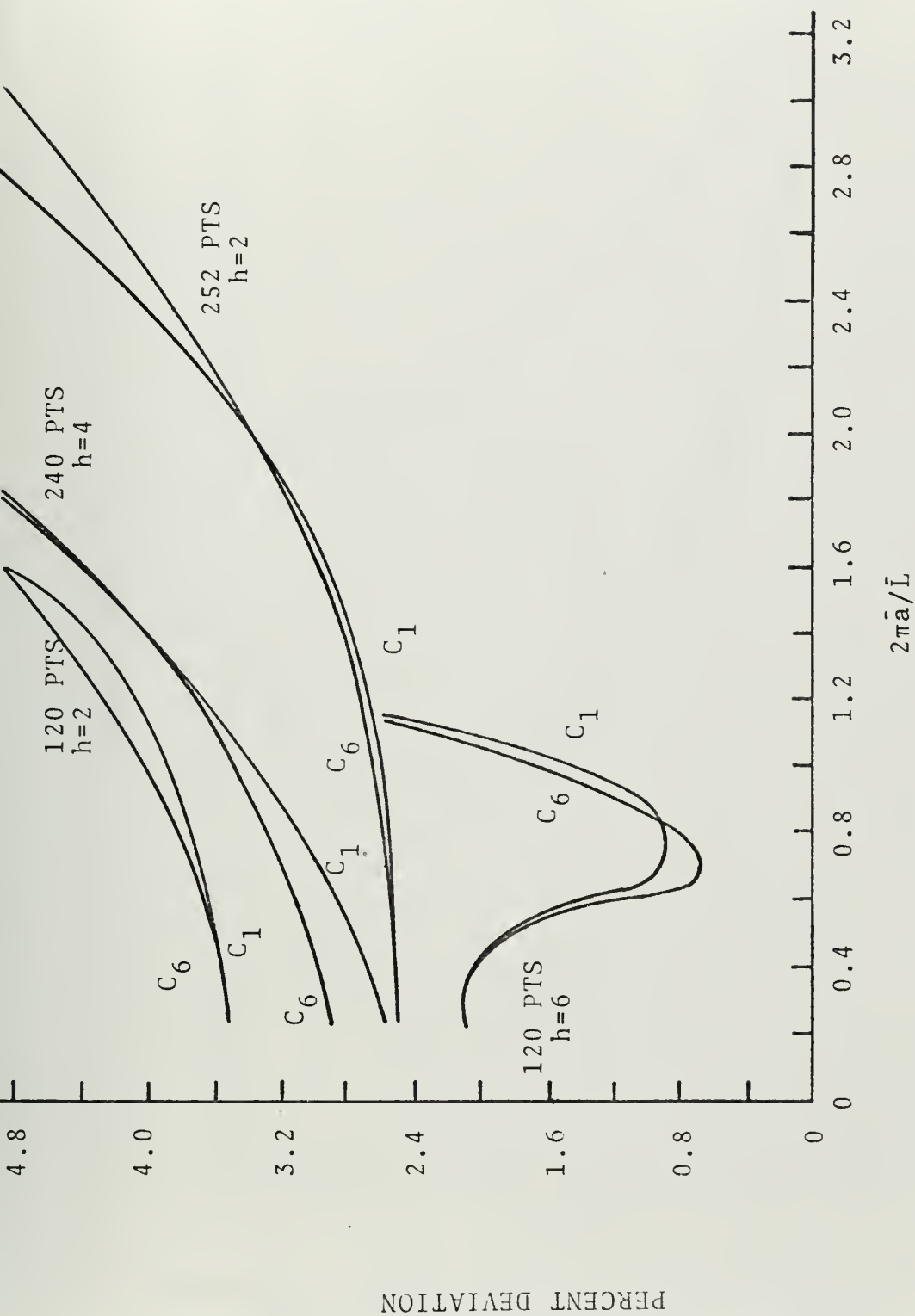


Figure 19: PERCENT DEVIATION OF HASKIND'S RELATIONS FROM
DIFFRACTION THEORY FOR A VERTICAL CIRCULAR CYLINDER

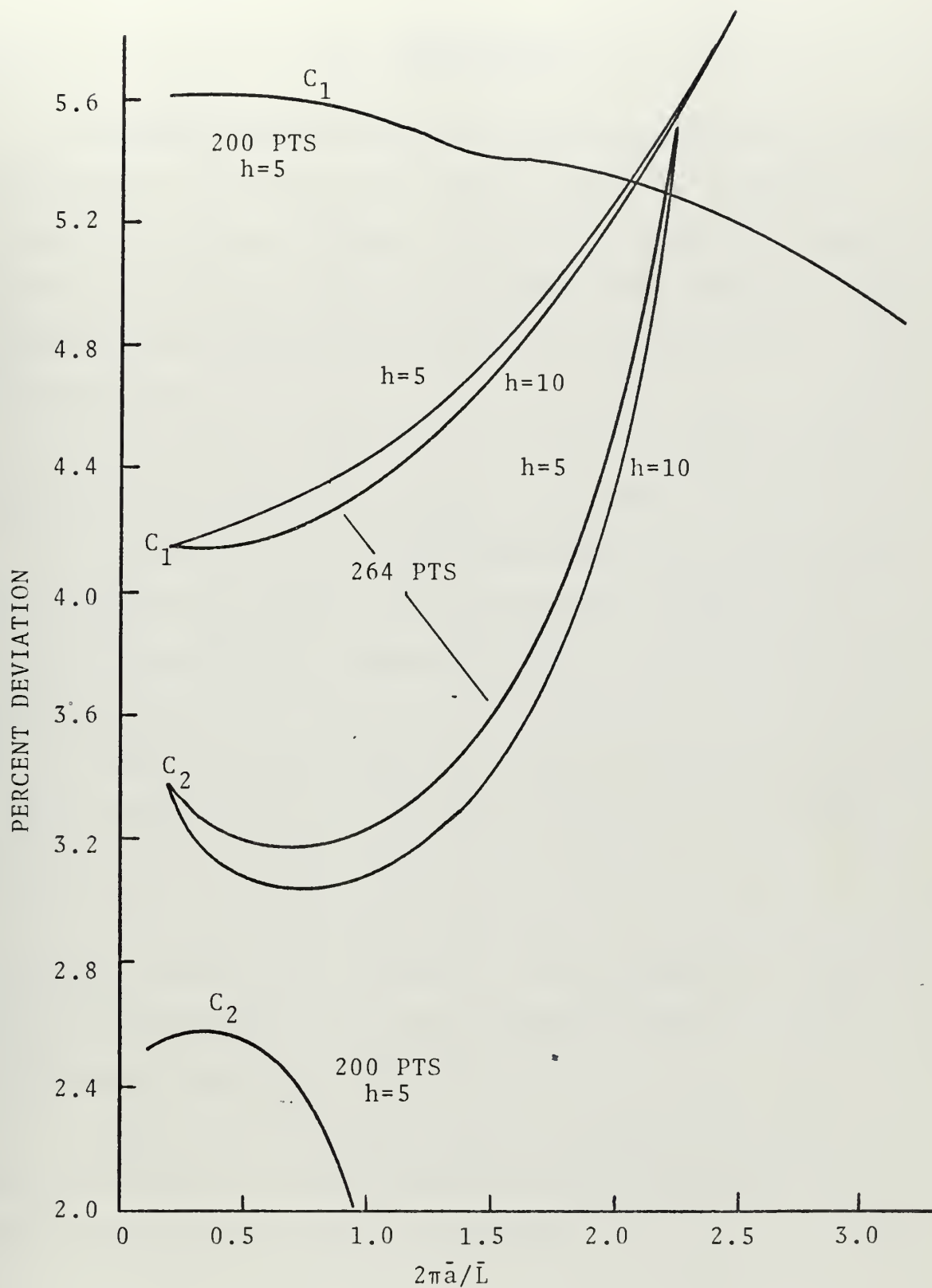


Figure 20: PERCENT DEVIATION OF HASKIND'S RELATIONS FROM DIFFRACTION THEORY FOR A SPHEROID

V. CONCLUSIONS

A computer program based on linear wave theory has been developed to calculate wave forces acting on submerged objects of arbitrary shape. In order to reduce the computation time, the restriction of symmetry with respect to two planes passing through the center of the object was incorporated.

On the basis of the results presented in Section IV, the following conclusions appear justified:

1. All of the checks and comparisons were successful and therefore it appears that the present method yields accurate results up to approximately $a = 3.0$ depending on the grid size.
2. The horizontal force and moment coefficients in all cases increase with the wavelength parameter a , at first, reach a peak and then decrease as a increases.
3. The vertical force coefficient for a floating spheroid starts with a value of π , corresponding to zero size to wavelength ratio, and decreases rapidly at first and later slowly as a increases.
4. Haskind's relations and the energy check give valuable checks on the accuracy and show the effect of increasing the grid size or the depth.

APPENDIX

HASKIND'S RELATIONS AND ENERGY CHECK

A. HASKIND'S RELATIONS

The dimensionless wave force and moment components, $F_i(t)$, on an object of arbitrary shape may be obtained by substituting for P' from (16) and (17) in (32) and simplifying. For the diffraction problem, this gives

$$F_i(t) = \text{Re} \left[a \iint_S (u_7 + u_0) \frac{\partial u_i}{\partial n} ds e^{-i\sigma t} \right], \quad i = 1, 2, \dots, 6 \quad (\text{A.1})$$

where u_i denotes the radiation potentials.

The scatter potential can be eliminated from (A.1) through the application of Green's reciprocal theorem, applied to G and u_j as

$$\iiint_R [u_j(x, y, z) \nabla^2 G(x, y, z; \xi, \eta, \zeta) - G(x, y, z; \xi, \eta, \zeta) \nabla^2 u_j(x, y, z)]$$

$$dx dy dz = \iint_{s_f + s_b + s_\infty + s} [u_j(x, y, z) \frac{\partial G}{\partial n}(x, y, z; \xi, \eta, \zeta)$$

$$- G(x, y, z; \xi, \eta, \zeta) \frac{\partial u_j}{\partial n}(x, y, z)] ds,$$

in the region R , as shown in Fig. 21. Since an incompressible fluid was assumed, both u_7 and u_i satisfy the Laplacian in the region R , Eq. (18a),

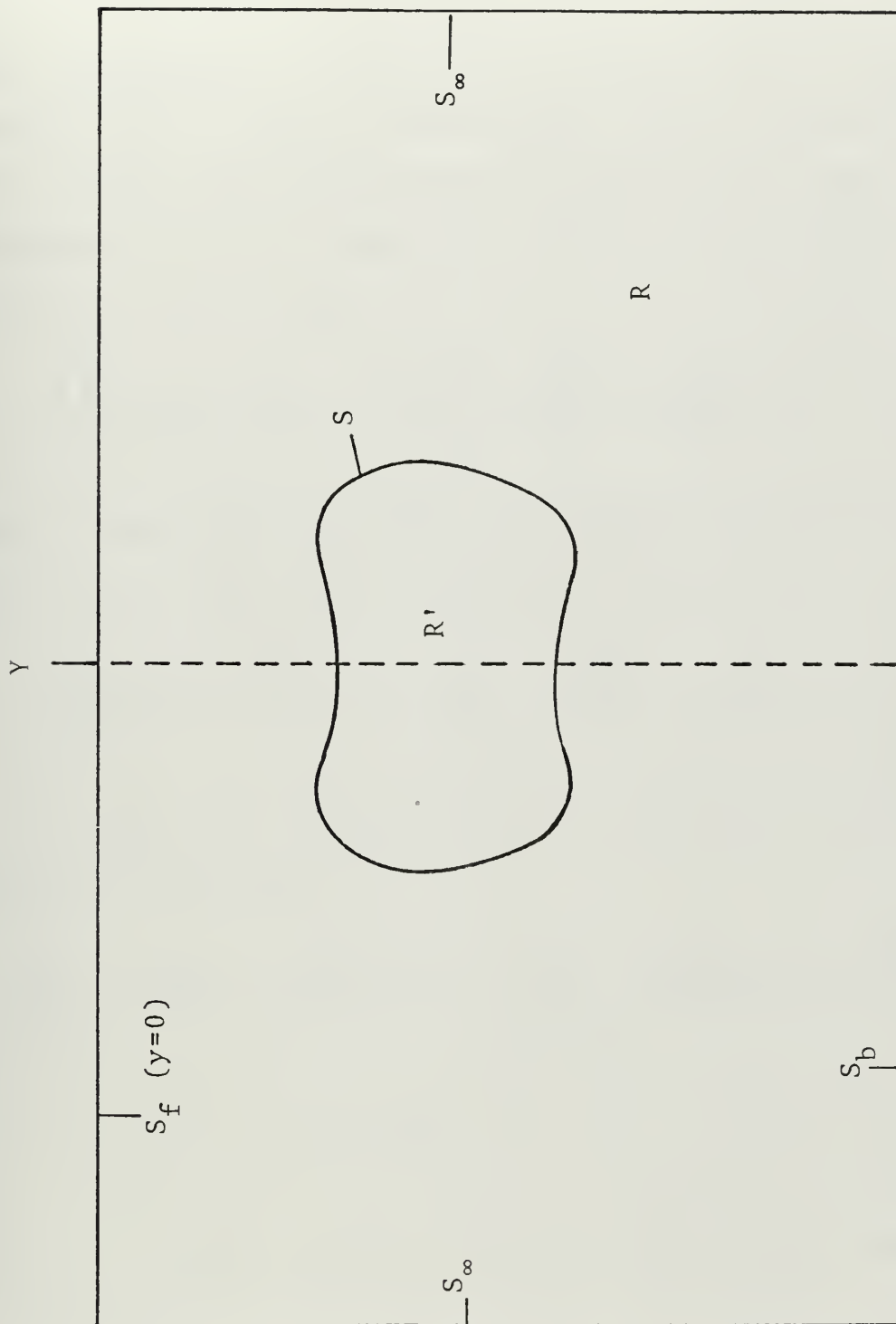


Figure 21: REGION OF APPLICATION OF GREEN'S THEOREM

$$\iint_{s+s_f+s_b+s_\infty} (u_i \frac{\partial u_7}{\partial n} - u_7 \frac{\partial u_i}{\partial n}) ds = 0 \quad (A.2)$$

The contributions to the surface integral in (A.2) from the surfaces S_f , S_b and S_∞ vanish since u_7 and u_i satisfy the free surface and bottom boundary conditions and the radiation condition at $R = \infty$. Also, from (18d) in conjunction with (14) and (15), (A.2) yields

$$\iint_s (u_7 + u_o) \frac{\partial u_i}{\partial n} ds = \iint_s (u_o \frac{\partial u_i}{\partial n} - u_i \frac{\partial u_o}{\partial n}) ds. \quad (A.3)$$

Again using Green's theorem, the surface integral on the right hand side of (A.3) may be replaced, thus giving

$$\iint_s (u_7 + u_o) \frac{\partial u_i}{\partial n} ds = - \iint_{s_\infty} (u_o \frac{\partial u_i}{\partial n} - u_i \frac{\partial u_o}{\partial n}) ds. \quad (A.4)$$

By using the radiation condition (18e) and since $x = r \cos \theta$, it can be shown that

$$\begin{aligned} \iint_{s_\infty} (u_o \frac{\partial u_i}{\partial n} - u_i \frac{\partial u_o}{\partial n}) ds &= - \iint_{s_\infty} u_o u_i [i a r (1 - \cos \theta) \\ &\quad - \frac{1}{2r}] ds. \end{aligned} \quad (A.5)$$

Substituting for u_o and u_i from (14) and (15) and then simplifying

$$\iint_{s_{\infty}} (u_o \frac{\partial u_i}{\partial n} - u_i \frac{\partial u_o}{\partial n}) ds = - \frac{1}{a \cosh^2(ah)}$$

$$[\frac{\sinh(2ah)}{4ah} + \frac{h}{2}] e^{iar}$$

$$\int_0^{2\pi} D_i(\theta) r^{-1/2} [1/2 - iar(1 - \cos \theta)] e^{iar \cos \theta} d\theta \quad (A.6)$$

Inasmuch as $r \rightarrow \infty$ and $e^{iar \cos \theta}$ is a fluctuating quantity, the real part of (A.6) equals zero. Thus

$$\begin{aligned} & - \int_0^{2\pi} D_i(\theta) iar^{-1/2} (1 - \cos \theta) e^{iar \cos \theta} d\theta \\ & = -iar^{-1/2} e^{iar} \int_0^{2\pi} D_i(\theta) (1 - \cos \theta) e^{-iar(1 - \cos \theta)} d\theta \quad (A.7) \end{aligned}$$

Since $ar \gg 1$, the solution to the integral on the right hand side of (A.7) may be obtained by the method of stationary phase (Stoker [11]). Hence

$$\begin{aligned} & \int_0^{2\pi} D_i(\theta) (1 - \cos \theta) e^{-iar(1 - \cos \theta)} d\theta \\ & ar \rightarrow \infty \end{aligned} \quad (A.8)$$

$$= 2 \left(\frac{2\pi}{ar} \right)^{1/2} e^{i(\frac{\pi}{4} - 2ar)} D_i(\pi)$$

and after simplifying

$$\iint_{s_\infty} (u_0 \frac{\partial u_i}{\partial n} - u_i \frac{\partial u_0}{\partial n}) ds = i \left(\frac{2\pi}{a}\right)^{1/2} \frac{1}{\cosh^2(ah)} \left[\frac{\sinh(2ah)}{2a} + h \right] e^{i\frac{\pi}{4}} D_i(\pi) \quad (A.9)$$

From (A.1), (A.3), (A.4) and (A.9), simplification gives

$$F_i(t) = \text{Re} \left\{ -i \frac{(2\pi a)^{1/2}}{\cosh^2(ah)} \left[\frac{\sinh(2ah)}{2a} + h \right] e^{i(\frac{\pi}{4} - \sigma t)} D_i(\pi) \right\} \quad (A.10)$$

and taking the modulus on both sides gives

$$C_i = \frac{(2\pi a)^{1/2}}{\cosh^2(ah)} \left[\frac{\sinh(2ah)}{2a} + h \right] |D_i(\pi)|, \quad i = 1, 2, \dots, 6 \quad (A.11)$$

In actuality, (A.11) represents six different equations which are known as "Haskind's relations." They relate the i^{th} component wave force (or moment) coefficient to the waves produced at infinity by the object oscillating in the i^{th} mode.

B. ENERGY CHECK

Equation (31) represents the i^{th} component of the dynamic force (or moment) arising due to the j^{th} mode of oscillation of the object. In the case of the radiation problem, they may each be expressed as the sum of two components, one in phase with the acceleration and the other in phase with the velocity of the body in the form

$$F_{ij}(t) = -\bar{M}_{ij} \ddot{a}_j(t) - \bar{N}_{ij} \dot{a}_j(t), \quad i, j = 1, 2, \dots, 6 \quad (A.12)$$

where \bar{M}_{ij} represents the added mass (or added moment of inertia) and is defined, when compared to (34), (36) and (37),

as

$$\bar{M}_{ij} = -\rho \bar{a}^3 \operatorname{Re} \left[\iint_S u_j(x,y,z) h_i(x,y,z) ds \right], \quad \begin{matrix} i = 1, 2, 3 \\ j = 1, 2, \dots, 6 \end{matrix} \quad (\text{A.13a})$$

for a force and for a moment as

$$\bar{M}_{ij} = -\rho \bar{a}^4 \operatorname{Re} \left[\iint_S u_j(x,y,z) h_i(x,y,z) ds \right], \quad \begin{matrix} i = 4, 5, 6 \\ j = 1, 2, \dots, 6 \end{matrix}, \quad (\text{A.13b})$$

and \bar{N}_{ij} denotes the damping coefficients (in relation to energy transport) and is defined, when compared to (34), (36) and (37), as

$$\bar{N}_{ij} = -\rho \sigma \bar{a}^3 \operatorname{Im} \left[\iint_S u_j(x,y,z) h_i(x,y,z) ds \right], \quad \begin{matrix} i = 1, 2, 3 \\ j = 1, 2, \dots, 6 \end{matrix} \quad (\text{A.14a})$$

for a force and

$$\bar{N}_{ij} = -\rho \sigma \bar{a}^4 \operatorname{Im} \left[\iint_S u_j(x,y,z) h_i(x,y,z) ds \right], \quad \begin{matrix} i = 4, 5, 6 \\ j = 1, 2, \dots, 6 \end{matrix} \quad (\text{A.14b})$$

for a moment.

The dimensional force (or moment) component, in the i^{th} direction, on the oscillating body due to oscillations in the i^{th} mode may then be obtained from (A.12) by equating j to i . Since the forces and moments exerted by the body on the fluid are equal and opposite to these, the energy transmitted by the object to the surrounding fluid during one period is given by

$$E_i = - \int_0^T (1 \text{ or } \bar{a}) F_{ii}(t) \dot{X}_i(t) dt \quad (\text{A.15})$$

where \bar{a} is used for a force ($i = 1, 2, 3$) and the factor 1 for a moment ($i = 4, 5, 6$). After carrying out the integration,

(A.15) may be rewritten as

$$E_i = \pi \rho \sigma^2 \bar{a}^5 X_i^{\circ 2} N_{ii}, \quad i = 1, 2, \dots, 6 \quad (\text{A.16})$$

where N_{ii} denotes the dimensionless damping coefficient which is defined for a force as

$$N_{ij} = \frac{\bar{N}_{ij}}{\rho \sigma \bar{a}^4}, \quad \begin{array}{l} i = 1, 2, 3 \\ j = 1, 2, \dots, 6 \end{array}$$

and for a moment as

$$N_{ij} = \frac{\bar{N}_{ij}}{\rho \sigma \bar{a}^4}, \quad \begin{array}{l} i = 4, 5, 6 \\ j = 1, 2, \dots, 6. \end{array}$$

If η_i° is the amplitude of the outgoing progressive waves at S_{∞} due to oscillation of the body in the i^{th} mode, then this amplitude can be related to the asymptotic velocity potential, u_i , by using the dynamic free surface boundary condition and

$$\eta_i^{\circ}(r, \theta) = \bar{a} X_i^{\circ} \tanh(kh) a |u_i(r, \theta, 0)|. \quad (\text{A.17})$$

The total energy transmitted over one period can now be written

$$E_i = \lim_{\bar{r} \rightarrow \infty} \frac{\rho \bar{L}}{4} \left[1 + \frac{2k\bar{h}}{\sinh(2k\bar{h})} \right] \frac{\bar{a}^4 \sigma^4}{g} X_i^{\circ 2} F \int_0^{2\pi} |u_j(r, \theta, 0)|^2 d\theta, \quad i = 1, 2, \dots, 6. \quad (\text{A.18})$$

Now, by comparing (A.16) and (A.18), the damping coefficients may be written in terms of the asymptotic velocity

potential, u_i , as

$$N_{ii} = \lim_{r \rightarrow \infty} \frac{1}{2} \tanh(ah) \left[1 + \frac{2ah}{\sinh(2ah)} \right] \int_0^{2\pi} |u_i(r, \theta, 0)|^2 d\theta, \quad i = 1, 2, \dots, 6. \quad (A.19)$$

C. NUMERICAL EVALUATION OF HASKIND'S RELATIONS AND ENERGY CHECK

The right hand sides of (A.11) and (A.19), involving the asymptotic velocity potentials, are solved by the use of the distribution functions f_i , obtained from the numerical solution of the radiation problem, in conjunction with the series form of Green's function (24).

For $r_1 \rightarrow \infty$ and $y = 0$, considerable simplification is possible in the asymptotic form of G and may be written as

$$G(x, 0, z; \xi, \eta, \zeta) = - \frac{2\pi(a^2 - v^2)}{a^2 h - v^2 h + v} \cosh(ah) \cosh[a(\eta + h)] \left(\frac{2}{\pi a r_1} \right)^{1/2} e^{i(ar_1 - \pi/4)}. \quad (A.20)$$

Thus the asymptotic potential, u_i , is given by

$$u_i(r, \theta, 0) = - \frac{i}{2} \left(\frac{2}{\pi a} \right)^{1/2} \frac{(v^2 - a^2) \cosh(ah)}{a^2 h - v^2 h + v} \iint_s f_i(\xi, \eta, \zeta) \cosh[a(\eta + h)] \bar{r}_1^{1/2} e^{i(ar_1 - \frac{\pi}{4})} ds. \quad (A.21)$$

Since it is large, r_1 may be replaced by r and moved outside the integral. Further, as shown in Fig. 22, for large r

$$r_1 = r - \rho_1 \cos(\beta - \theta)$$

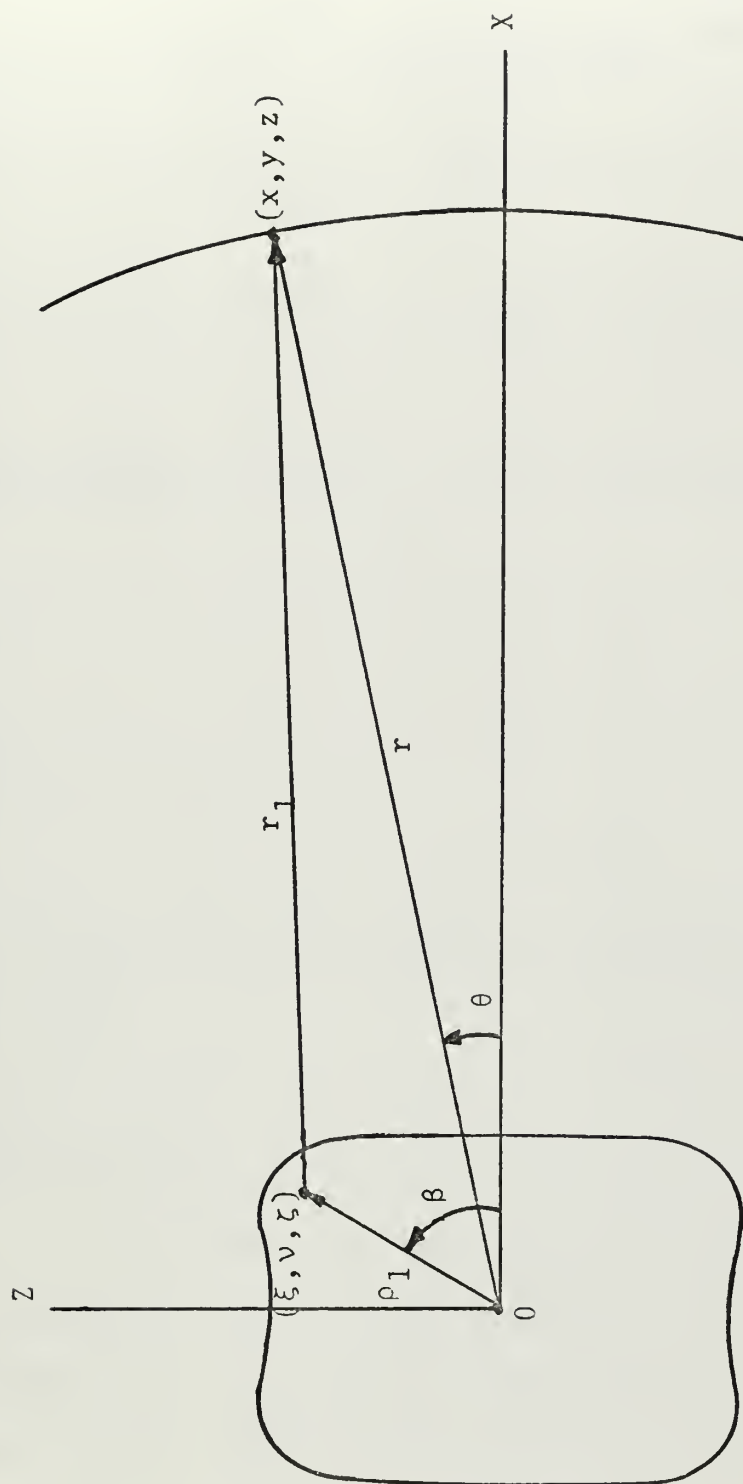


Figure 22: PLAN VIEW OF THE OBJECT

where $\rho_1 = (\xi^2 + \zeta^2)^{1/2}$, and u_i may be rewritten as

$$u_i(r, \theta, 0) = -i(2a)^{-1/2} \frac{(v^2 - a^2) \cosh(ah)}{a^2 h - v^2 h + v} r^{-1/2} e^{i(ar - \frac{\pi}{4})} \iint_S f_i(\xi, \eta, \zeta) \cosh[a(\eta+h)] \bar{e}^{ia\rho_1 \cos(\beta-\theta)} ds. \quad (A.22)$$

Substituting (A.22) into (A.19) and simplifying gives the result

$$N_{ii} = \frac{1}{2\pi} \left[\frac{a^2 - v^2}{a^2 h - v^2 h + v} \right] \int_0^\pi \left| \iint_{1/2S} f_i(\xi, \eta, \zeta) \cosh[a(\eta+h)] (e^{-ia\rho_1 \cos(\beta-\theta)} + e^{-ia\rho_1 \cos(\beta+\theta)}) ds \right|^2 d\theta. \quad (A.23)$$

Once $u_i(r, \theta, 0)$ is known, $D_i(\pi)$ may be obtained by using the radiation condition (18e). Thus

$$D_i(\pi) = u_i(r, \pi, 0) r^{1/2} e^{iar} \quad (A.24)$$

and after simplifying by means of trigonometric identities, (A.11) becomes

$$C_i = \frac{2}{\cosh(ah)} \iint_{1/2S} f_i(\xi, \eta, \zeta) \cosh[a(\eta+h)] e^{-ia\pi_1 \cos(\beta-\pi)} ds, \quad (A.25)$$

where $i = 1, 2, \dots, 6$ since for an axisymmetric body, the only cases of interest are those pertaining to $i = 1, 2$, and 6 .

A comparison of the results obtained from (A.23) and (A.25) with those calculated by integration of the pressure over the submerged surface, Eqs. (37) and (38), are a valuable self-check on the accuracy of the numerical results.

LIST OF REFERENCES

1. Sarpkaya, T., and C. J. Garrison, "Vortex Formation and Resistance in Unsteady Flow," Journal of Applied Mechanics Transactions of the ASME, v. 30, series E, no. 1, p. 16-24, March 1963.
2. Garrison, C. J., and V. Seetharama Rao, "Interaction of Waves with Submerged Objects," Journal of Waterways, Harbors and Coastal Engineering Division Proceedings of the ASCE, v. 97, no. WW2, p. 259-277, May 1971.
3. Wehausen, J. V., and E. V. Laitone, "Surface Waves," Encyclopedia of Physics, ed. S. Flugge, v. 9, Fluid Dynamics III, Springer-Verlag, p. 478, 1960.
4. Seetharama Rao, V., Interaction of a Train of Regular Waves with a Rigid Submerged Ellipsoid, Ph.D. Thesis, Texas A & M University, 1971.
5. Garrison, C. J., "On the Interaction of an Infinite Shallow Draft Cylinder Oscillating at the Free Surface with a Train of Oblique Waves," Journal of Fluid Mechanics, v. 39, p. 227-255, 1969.
6. MacCamy, R. C., and R. A. Fuchs, "Wave Forces on Piles: A Diffraction Theory," Beach Erosion Board, Technical Memorandum, no. 69, 1954.
7. Havelock, T., "Waves due to a Floating Sphere Making Periodic Heaving Oscillations," Proceedings of the Royal Society, London, England, v. 231, series A, p. 1-7, July 1955.
8. Kim, W. D., "On the Harmonic Oscillations of a Rigid Body on a Free Surface," Journal of Fluid Mechanics, v. 21, p. 427-451, 1965.
9. Kim, W. D., "On a Free-Floating Ship in Waves," Journal of Ship Research, v. 10, p. 182-200, September 1966.
10. Milgram, J. H., and J. E. Halkyard, "Wave Forces on Large Objects in the Sea," Journal of Ship Research, v. 15, p. 115-124, June 1971.
11. Stoker, J. J., Water Waves, Interscience Publishers, New York, 1957.

INITIAL DISTRIBUTION LIST

	No. Copies
1. Defense Documentation Center Cameron Station Alexandria, Virginia 22314	2
2. Library, Code 0212 Naval Postgraduate School Monterey, California 93940	2
3. Asst Professor C. J. Garrison, Code 59 Gm Department of Mechanical Engineering Naval Postgraduate School Monterey, California 93940	3
4. Mr. Raymond Gardiner Quaintance 6410 Fifteenth Street Alexandria, Virginia 22307	1
5. LT Peter K. Bowden, USN 117 Russell Street Peabody, Massachusetts 01962	2
6. Department of Mechanical Engineering, Code 59 Naval Postgraduate School Monterey, California 93940	1

UNCLASSIFIED

Security Classification

DOCUMENT CONTROL DATA - R & D

(Security classification of title, body of abstract and indexing annotation must be entered when the overall report is classified)

ORIGINATING ACTIVITY (Corporate author)

2a. REPORT SECURITY CLASSIFICATION

Unclassified

2b. GROUP

Naval Postgraduate School
Monterey, California 93940

REPORT TITLE

Wave Interaction with Large Submerged Objects

DESCRIPTIVE NOTES (Type of report and, inclusive dates)

Master's Thesis; December 1971

AUTHOR(S) (First name, middle initial, last name)

Peter Klaus Bowden

REPORT DATE

December 1971

7a. TOTAL NO. OF PAGES

71

7b. NO. OF REFS

11

a. CONTRACT OR GRANT NO.

9a. ORIGINATOR'S REPORT NUMBER(S)

b. PROJECT NO.

9b. OTHER REPORT NO(S) (Any other numbers that may be assigned this report)

c.

d.

10. DISTRIBUTION STATEMENT

Approved for public release; distribution unlimited.

11. SUPPLEMENTARY NOTES

12. SPONSORING MILITARY ACTIVITY

Naval Postgraduate School
Monterey, California 93940

13. ABSTRACT

The practical and rigorous solutions of the potential problem associated with the harmonic oscillation of a submerged rigid body of arbitrary shape is presented. The use of Green's function reduces the determination of the potential to the solution of an integral equation. The integral equation is solved numerically and the dependency of the hydrodynamic quantities such as added mass and damping coefficients of the object on the frequency of the oscillation is established.

Several checks are made on the numerical results. These include the Haskind's relations check, an energy check for the radiation problem, and comparisons with closed form solutions. All the checks and comparisons are successful and it appears that the numerical procedure employed yields valid and accurate results.

Diffraction Theory

Wave Forces

Haskind's Relations

24 JUL 72

19730

133524

Thesis

B7387

Bowden

c.1

Wave interaction with
large submerged objects.

24 JUL 72

19730

Thesis

B7387

Bowden

c.1

Wave interaction with
large submerged objects.

133524

thesB7387

Wave interaction with large submerged ob



3 2768 002 07360 3

DUDLEY KNOX LIBRARY